

FIRST WALL THERMAL ANALYSIS OF A TOKAMAK REACTOR

*A thesis submitted
in Partial fulfilment of the requirements
for the award of the degree of
MASTER OF TECHNOLOGY*

**BY
DEBASISH MISHRA**

to the
**NUCLEAR ENGINEERING AND TECHNOLOGY PROGRAMME
INDIAN INSTITUTE OF TECHNOLOGY, KANPUR
February-93**

08 APR 1993

NET

CENTRAL LIBRARY
I I T., KANPUR

Acc. No. A. 115444

Th

621.483

M 687 f

NETP-1993-M-MIS-FIR

CONTENTS

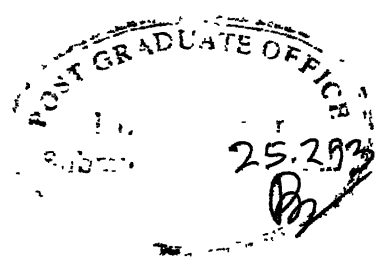
TITLE	PAGE NO.
CERTIFICATE	i
ABSTRACT	ii
ACKNOWLEDGEMENTS	iii
CHAPTER 1 INTRODUCTION (AND FIRST WALL)	1
1.1 Introduction	1
1.2 Tokamak and first wall	2
1.3 System code for tokamak	7
1.4 Earlier work	8
1.5 Present work	8
CHAPTER 2 THEORITICAL MODEL	11
2.1 A brief outline of the method followed	11
2.2 Details of source terms	15
2.2.1 Bremsstrahlung radiation	15
2.2.2 Cyclotron radiation	23
2.2.3 Charge exchange neutrals	25
2.2.4 Line radiation	27
2.2.5 Fusion neutrons	30
2.3 Calculation algorithm for local wall loading	31
2.3.1 Volumetric heat generation terms	35
2.4 Temperature solution in the first wall	37
2.5 Limitations and suggestions in the model	40
CHAPTER 3 SYSTEM CODE FOR FIRST WALL TEMPERATURE CALCULATION	
3.1 A brief outline about the code	43
3.2 Input / output of the code	44
3.3 Flow chart	46

CHAPTER 4 RESULTS

47

REFERENCES

67



CERTIFICATE

It is to certify that the work contained in the thesis titled 'FIRST WALL THERMAL ANALYSIS OF A TOKAMAK REACTOR' has been carried out under our supervision and that this work has not been submitted elsewhere for the award of a degree.

K. Sri Ram
K. Sri Ram)

Professor
Mechanical Engg. &
Technology Programme,
IIT Kanpur

S. Chaturvedi
(Dr. S. Chaturvedi)

Institute for Plasma
Research, Bhat
Gandhinagar

ABSTRACT

The main objectives of this study is to develop a computer code that can assess the performance of the thermal parameters of the first wall during the steady state normal operation of the "ADITYA" (The Indian tokamak).

A thermal analysis model is presented on the basis of which a code is developed. The code is capable of calculating the temperature profile in the first wall. Most of the parameters required for these calculation are inbuilt within the code. Two types of density and temperature profile of electron and ion are considered.

Poloidal distribution of the thermal flux (Due to bremsstrahlung, cyclotron, charge exchange, line radiation, and neutron) are calculated, with the assumption of a specific coolant arrangement system this is then coupled to a one dimensional heat conduction equation to derive the temperature profile in the first wall.

ACKNOWLEDGEMENTS

I express my deep sense of indebtedness and gratitude to Dr K. Sri Ram and Dr Shashank Chaturvedi for their guidance, encouragement and criticism at all stage of work. I take this opportunity to thank Dr M. S. Kalra for his valuable suggestions during the work.

I am thankful to Dr Prabhat Munshi and Dr A.Sengupta for their inspiring teaching during the course work.

I am thankful to all faculty members ,Library staff of Institute for Plasma Research ,Bhat,Gandhinagar, and in particular to my friends Raju, Amar Das, Pradhan and Jana for the love affection and help I got during my stay at I.P.R.

I am indebted to my friends Barada, Satyabrata, J.S.Murty, Lt Asok, Y.P., Rakesh and Sanjeev for making my stay here a pleasant one.

I am thankful to Dr Pradeep Kumar and Krishna Mohan for their needful help.

I wish to thank all NET staff for their cooperation and fairness.

I wish to express my gratitude to my parents for their love, affection and encouragements.

Finally a special thanks to Anjali for the love, care and encouragement throughout this work.

February-1993

DEBASISH MISHRA

CHAPTER 1

INTRODUCTION (AND FIRST WALL PERFORMANCE)

1.1 Introduction:

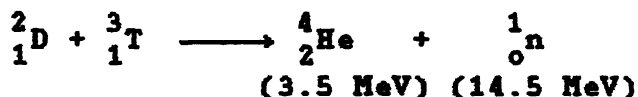
Thermonuclear fusion research is making rapid progress around the world. Tokamaks have so far yielded best results amongst the various magnetic confinement schemes under study. The Joint European Torus (JET), has recently reported conditions very close to those required for break-even. Preliminary design studies have already been completed for the next generation tokamak called ITER (International Thermonuclear Experimental Reactor). Fusion reactors meant for electric power tend to be big and expensive. The first commercial application of tokamaks in India is likely to be as a low gain source of fusion-neutrons for fissile fuel production. Study of a fusion breeder is underway at the Institute for Plasma Research (IPR), Bhat, Gandhinagar (India).[1] Objectives included in the programme are, determination of the tokamak and blanket parameters required for the device and a study of how these devices could fit into the Indian nuclear power programme. The programme at IPR. is divided into two types, i.e. short-term and long term objectives. In the short term objective main emphasis is on a low fissile - production rate (FPR ~ few kg/year) and reducing cost, simplifying design. The device is intended to demonstrate the feasibility of fusion breeders. The long term objective is a scale-up of the first. It will have a moderate FPR (few hundred kg/year). Its larger size and more complex design will increase the energy gain to a level that is energetically attractive.

Some intermediate steps are necessary between the currently existing Indian tokamak 'ADITYA' and the final device. Work is in progress for determining the optimal parameters of the intermediate steps.

1.2 Tokamak and First Wall

Tokamak [2-5]

If a nucleus of a deuterium fuses with a nucleus of a tritium an α -particle is produced and a neutron is released. The nuclear rearrangement results in a reduction of total mass and a consequent release of energy in the form of kinetic energy of the reaction products.



In order to produce the fusion of nuclei of deuterium and tritium it is necessary to overcome the mutual repulsion due to their positive charges. Fusion brought about by heating the nuclei to a high temperature is called thermonuclear reaction. The temperature required to start fusion is approximately of the order of 10 KeV ($\sim 10^8$ K). At such temperature the fuel (D & T) is fully ionized. The neutral gas thus formed is called plasma.

A tokamak is a device, where this plasma particles are confined to a toroidal region by a magnetic field. In a tokamak it is necessary to confine the energy of a sufficiently dense plasma for a time which allows an adequate fraction of the fuel to react.

In a tokamak at the required ion-density of around 10^{20} m^{-3} , this confinement time should be around 1.5 sec. [5]. The product

of ion density and confinement time is often known as Lawson criteria, which says, the energy output from the fusion will be greater than energy input if the product of ion-density and confinement time is around $(1.5-3) \times 10^{20} \text{ m}^{-3} \text{ sec.}$ (when temperature is around 10 ~ 20 KeV) [4].

The principal magnetic field in a tokamak is the toroidal field, however this field alone does not allow confinement of plasma. In order to have an equilibrium between the plasma pressure and magnetic pressure, it is necessary to provide a poloidal field. Poloidal field coils are used for this purpose, but mainly the plasma current contributes to the poloidal field.

The layout of principal components in a conceptual tokamak reactor is shown in Fig. 1.1 and 1.2.

The core is magnetically confined plasma. Moving radially outward the next feature is the limiter or a divertor (not shown in Fig). The main use of limiter is to scrape off and remove impurities and fuel ions from the surface of the plasma as they move outward but before they can hit and damage the first wall. Divorter plays the same role as the limiter, the difference is that diverters are magnetic limiter, there exist a diverter current to produce suitable magnetic field which guides the escaping plasma particles to a separate chamber where the particles are neutralized and pumped away. An annular insulating vacuum region separates the plasma from the first wall. The first wall (sometime known as the vacuum wall) is the material surface that faces the plasma and through which the neutrons and also the radiant energy flux passes. Behind the first wall are

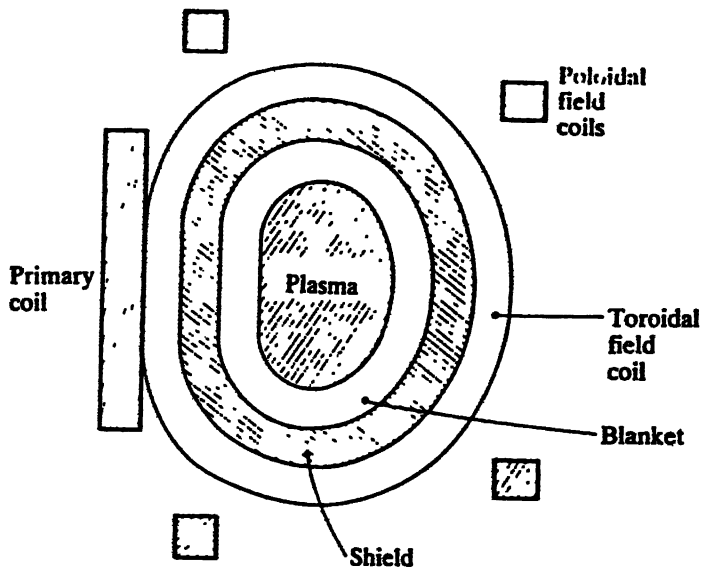


Fig. 1.1

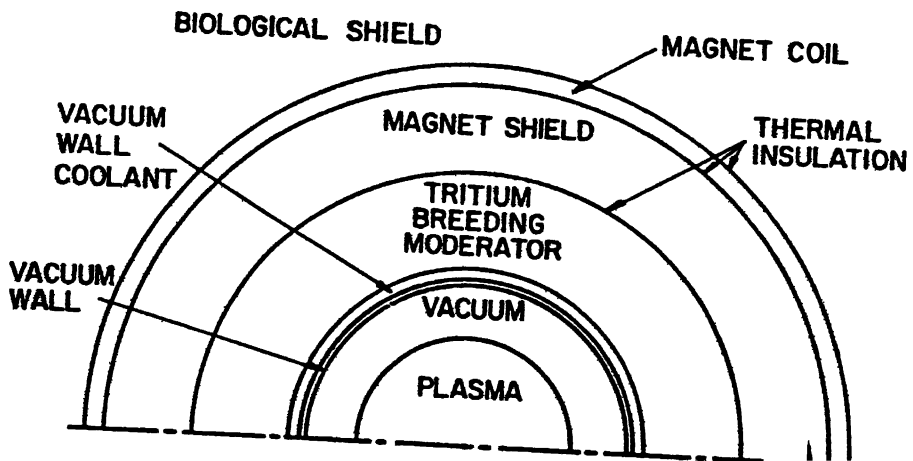
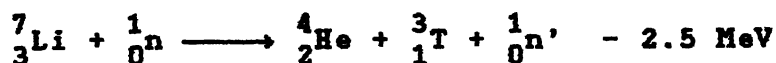
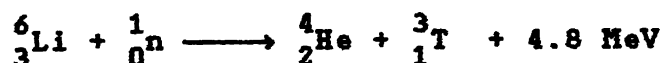


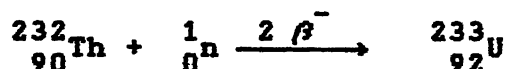
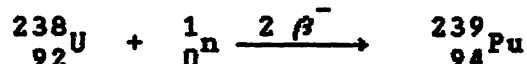
Fig. 1.2

Layout of a conceptual Tokamak 1

coolant passages designed to remove the thermal heat loading from radiations and particle bombardment. Beyond the first wall is a blanket, which in D-T reactors contains lithium to breed the required tritium fuel. In fissile fuel breeder type tokamak, this blanket contains suitable material, which after reacting with the fusion neutrons produces fissile material.



Blanket thicknesses of around 1 m. are required to moderate and absorb 14 MeV neutrons and to produce required amount of tritium or fissile material. Typical breeding reactions are:



Beyond the blanket is a magnetic thermal shield, which slows down and absorbs neutrons. The superconducting magnetic coils are next major systems in the reactor. Outside the superconducting magnetic coils a biological shield is present to reduce radiation to low enough level that maintenance personnel can approach the exterior of the reactor.

First Wall [2-5]

The first wall of a tokamak reactor and its associated structures operate in a severe environment like

1. Neutron released in the fusion reaction and the charge exchanged neutrals the wall

2. The wall is subjected to a very high pressure difference, i.e. the side facing plasma is at vacuum and other side at normal pressure.

3. Heating from one end (side facing the plasma) and cooling of the outer side.

Because the life of first wall depends on fluence of neutrons, thermal energy and charged particles in a tokamak, and there is a strong motivation to increase these fluxes to their maximum possible values, so there is a necessity of reaching an optimum balance between allowable wall loadings and first wall lifetime.

The first wall consists of a chamber that contains the plasma and the associated structures. The associated structures include limiters or diverters, and low Z-material coating. The diverters perturb the confining magnetic field, in a way so that the escaping fuel ions impinge in a controlled way on the diverter plates, usually remote from the first wall. A wide variety of first wall material has been reported in literature. The mostly used material is generally S.S. - 316 or S.S. - 314 type. The exact dimensions of first wall depends on other tokamak parameters, however the thickness lies between 1 cm-2 cm.

The functions of the first wall are:

1. To remove heat caused by bremsstrahlung and synchrotron or cyclotron radiation, by fusion neutrons and by fusion reaction products which bombards the first wall.
2. It copes with the charged particles and charge-exchanged energetic particle fluxes that arise in the plasma and

deposited on the first wall.

3. The first wall deals with localized energy deposition resulting from plasma disruptions or run away electrons. Because of these processes the plasma dumps a significant fraction of the plasma energy on the surface of the first wall.
4. The first wall designed in a manner so as to reflect back most of the cyclotron radiation into the plasma, hence prevent cooling of plasma rapidly.

1.3 System Code for Tokamak [7]

A computer code is needed for integrated modelling of the tokamak. Such a system code is required for the following reasons:

1. A tokamak based breeder has a large number of free parameters, along with a number of constraints. It is necessary to determine a wide range of optimal parameter sets from the point of view of cost as well as required parameters of sub-system. This can only be done by a system code.
2. At different stages of the design it may be necessary to introduce new information and constraints. The code will then be required to determine the revised optimal parameters.

A systems code allows a wide range of parameter sets to be examined within a reasonable time frame, and the optimal set to be selected. Estimates of system costs are, however only approximate. On the other hand, a detailed design gives accurate values for the cost and parameter values, but is expensive in

terms of computational time and effort. Hence two approaches are complementary.

1.4 Earlier Work

Systems codes already exist, and have been used extensively for conceptual designs of many tokamaks through out the world. Several laboratories have indicated that they are unable to transfer their codes due to variety of reasons [7]. Hence the need for developing a code.

A multi code consisting essentially of three modules, the 'first wall', the 'neutral gas' and the 'plasma' module is developed by A. Nicolai and D. Reiter [8]. The first wall module contains the thermal aspects of the first wall; on the basis of implantation of charge exchange neutrals and ohmic heating only.

M.C. Carroll and G.H. Miley have reported a model for first wall thermal response [9]. They have not considered the effect of line radiation and radiative recombination radiations from the impurities present in the plasma as a source of heating of first wall.

M.C. Carroll in his Ph.D. theses [10] developed a very accurate method to compute the local wall power loading, using the toroidal correction factors. A polynomial fit formula with data are available to correct the local wall power loading for toroidal curvature.

1.5 Present Work

The main objective of this study is to develop a computer

code that can assess the performance of thermal parameters of the first wall during normal operation of the 'ADITYA' tokamak. The term 'normal' denotes conditions under which plasma parameters vary in a controlled manner. This is different from the plasma 'disruption' where the energy of the plasma is dumped at the first wall in a very short period of time. Normal operation is however not restricted to a steady-state operation, but the code developed here is assuming a steady-state normal operation only.

A thermal analysis model is presented on the basis of which a code is developed. With some fundamental tokamak parameters as input, the code can give the temperature in the first wall - as a function of (x, θ) , where x is the depth into the first wall material and ' θ ' is the poloidal angle. Most of the parameters, like various reaction rates, are inbuilt within the code, and for different input conditions, these reaction rates are automatically evaluated from suitable polynomial fits discussed later.

The code can be used for two types of profiles of density and temperature, i.e. flat type and peaked type.

Plasma considered inside the tokamak is of Deuterium and Tritium 50% mixture. It is very difficult to obtain a 100% pure mixture of D & T for this purpose. Hydrogen is a common impurity in both D & T. Also because of erosion from the first wall which is made of S.S. - 314 (in some cases other grade of S.S. are used) which has high carbon contents material, significant amount of carbon impurities also lies within the plasma. It has been considered here that carbon and hydrogen are the two impurities

in the plasma of D & T. Existence of other impurity atoms however can not be ruled out, but to make the model simpler, only two types of impurities are considered. Since the code developed is in a modular fashion, inclusion of other impurities if necessary in future can be done with some minor modifications.

The torus cross section considered here is elliptical one, which is the case of "ADITYA". First wall material chosen is S.S. - 314. A specific combination of cooling arrangement of first wall is chosen i.e. water flowing in tubes attached to the back of the first wall, with one/two input and one/two output is considered.

This code can however be used for other type of torus cross-sectional geometry and coolant arrangement, because of its modular fashion.

CHAPTER 2

THEORETICAL MODEL

2.1 A Brief Outline of the Method Followed

In this chapter methods and equations are developed to execute the calculation sequence discussed in 2.3 and 2.4. Theoretical development not discussed in other references is described in more detail. Where other references [3-5] are involved, material is briefly reviewed for the sake of completeness. To adequately explain some of the numerical procedures, it was necessary to include calculational examples, which are included for "ADITYA" parameters using this model in Chapter 4.

A thermal analysis model, with corresponding solution methods has been developed for determining temperatures at the surface and interior of the first wall. Given the wall material and geometry, this model is capable of computing the local wall power loadings (including cyclotron, bremsstrahlung, charge exchange, line and radiative recombinations radiations, and fusion neutrons). The model encompasses a geometric analysis for determining loading variations along the poloidal angles and coupled with a one dimensional heat transfer analysis for determining temperatures in the first wall.

The two types of profile considered are flat type and peaked type. In a flat type of profile, the densities and temperature remains constant in the entire plasma cross section inside the torus

$n_{i,e} \quad T_{i,e}$ is constant.

The peaked type profile is assumed as:

$$T_{i,e}(r) = (T_{i,e})_0 (1 - r^2/a^2)^{\alpha_T} \quad (2.1)$$

$$n_{i,e}(r) = (n_{i,e})_0 (1 - r^2/a^2)^{\alpha_n} \quad (2.2)$$

where a = major radius of the plasma column.

α_T, α_n are constant.

The heat transfer problem analyzed is pictured in Fig. 2.1 [10-11]. Radiations, charge exchanged neutrals and fusion neutrons are emitted from the plasma. After passing through a vacuum, they impinge on the first wall. Charge exchanged neutrals, cyclotron radiation and line, radiative recombinations radiations deposit their energy at the surface of the wall, whereas bremsstrahlung and neutrons penetrate into the material of first wall; in the case of neutrons, it may pass through completely the wall. Heat from the energy deposition is conducted to the bulk of the coolant and is then carried out of the reactor to be converted to useful energy. So, the source terms, which are responsible for heating of first wall, is divided into two types, i.e. surface heating terms and volumetric heating terms. They are then treated separately for the temperature solution.

The sequence followed in this model is shown in block diagram in Fig. 2.2.

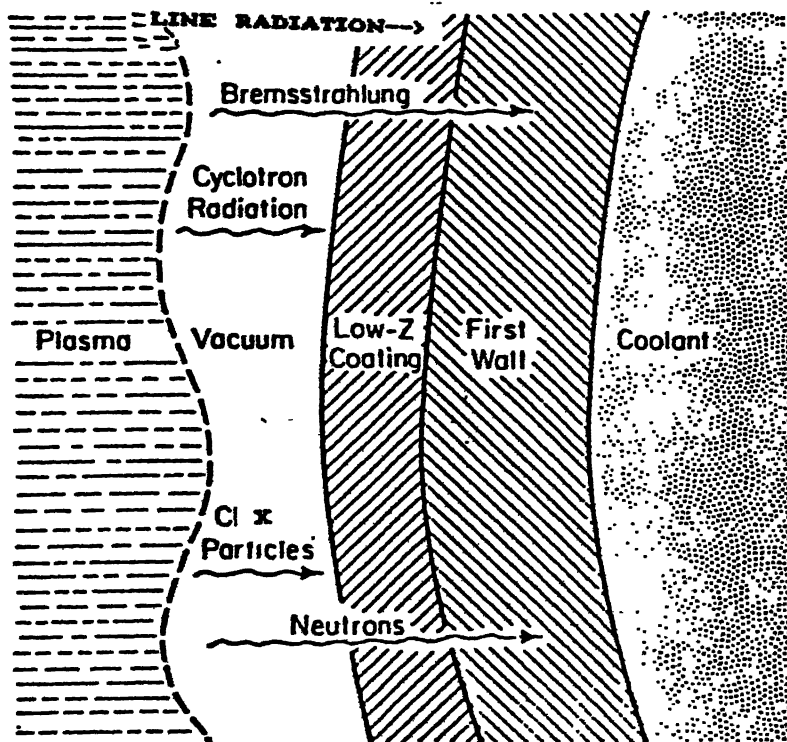


Fig 2.1 Sketch of the First-wall Heat Transfer Problem.

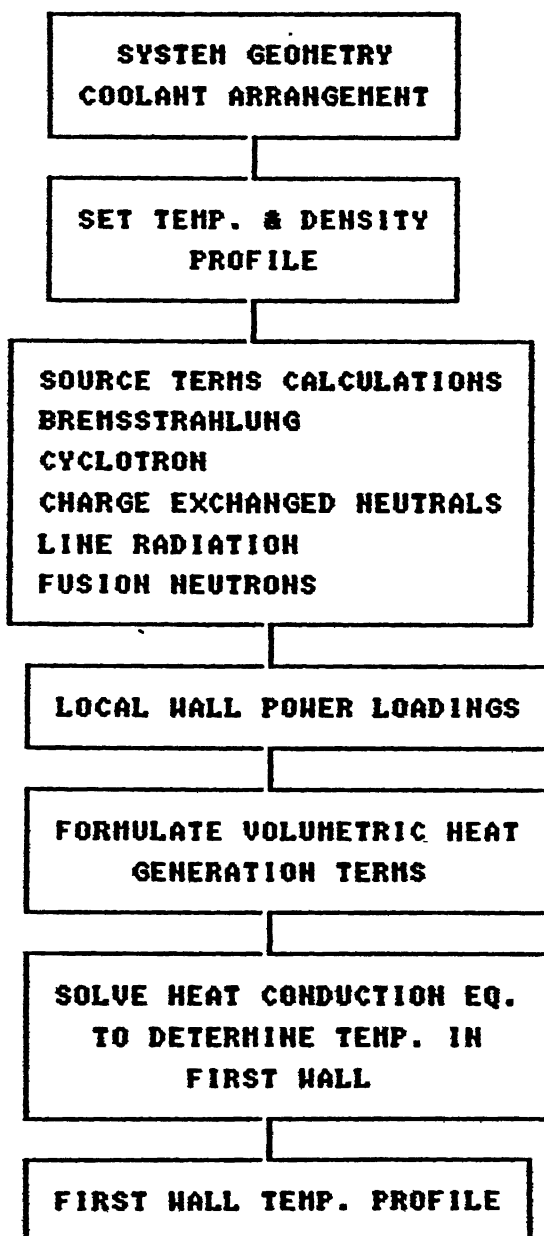


Fig 2.2

Calculation Sequence

2.2 Details of Source Terms

Different processes in the plasma which contribute significantly to the wall loading are

1. Bremsstrahlung radiation
2. Cyclotron radiation
3. Neutrals formation due to charge exchange mechanism
4. Line radiations
5. Fusion neutrons.

Details of these source terms are discussed below, with equations and procedure for their calculations.

2.2.1 Bremsstrahlung Radiation

This form of radiations occurs in a plasma when one particle encounters other and make a sudden change in direction. It is generally identified as a free-free transition radiation [12]. It constitutes an energy loss and cooling mechanism for the plasma which increases with the increase of proton number of the fuel species or impurities. Bremsstrahlung radiation is emitted in a continuous distribution of frequencies ranging from radio frequencies upto photons with energies several times the electron kinetic temperature. The average bremsstrahlung photon comes out of a plasma with an energy comparable to electron temperature of the plasma [3].

Since the electron temperature of a fusion plasma remains sufficiently high ($> 10 \text{ KeV} \sim 10^8 \text{ K}$) there is a negligible probability that these bremsstrahlung photons will be reabsorbed within the plasma. Such energetic photons are - absorbed by the

first wall without significant reflection from it.

A rigorous formulation for the bremsstrahlung radiation power loss can be developed by using quantum mechanics and treatment of relativistic effects [13]. But here, an approximate analysis and in a non-relativistic range is considered for the formulation of bremsstrahlung radiation.

From [3], total power 'p' in watts radiated from a single electron of charge 'e' moving with a velocity \underline{V} and acceleration $\dot{\underline{V}}$ is given by the formula:

$$\frac{dP}{dt} = \frac{e^2}{6\pi \epsilon_0 c^3} \frac{[|\dot{\underline{V}}|^2 - (\underline{V} \times \dot{\underline{V}})^2 / c^2]}{(1 - V^2/c^2)^3} U \quad (2.3)$$

In the non relativistic case

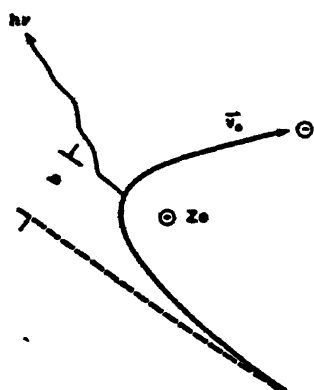
$$\frac{dp}{dt} = \frac{e^2 \dot{\underline{V}}^2}{6\pi \epsilon_0 c^3} U \quad (2.4)$$

Assuming an electron of charge 'e' is approaching a positive ion of charge 'Ze' with impact parameter 'b' and during the interaction the electron suffers a force which results in an emission of a photon of energy $h\nu$ (Fig. 2.3).

Average Coulomb force between the electron and the ion when separated by a distance 'b' impact parameter is

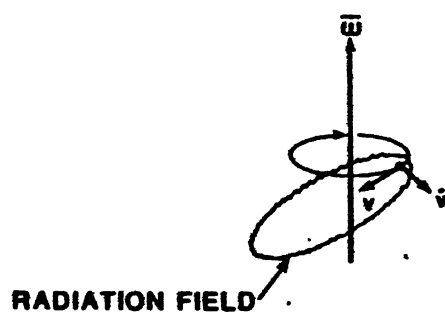
$$F = m_e \cdot \dot{\underline{V}} = \frac{Ze^2}{4\pi \epsilon_0 b^2} \quad (2.5)$$

Average acceleration of the electron, when it interacts with a ion of proton no. 'Z' is from (2.5)



Emission of a photon during the bremsstrahlung radiation process.

Fig 2.3



Electron gyrating in a strong magnetic induction and emitting synchrotron radiation along its velocity vector in the plane of its orbit.

Fig 2.4

$$\dot{\underline{v}} = \frac{Ze^2}{4\pi \epsilon_0 b^2 m_e} \quad (2.6)$$

Now (2.3) can be modified as,

$$\frac{dp}{dt} = \frac{Z^2 e^6}{96 \pi^3 \epsilon_0^3 c^3 m_e^2 b^4} \quad (2.7)$$

If the electron was in the vicinity of the ion for a time 't',

$$t = b/V \quad (2.8)$$

Radiation per collision is

$$E = t \times \frac{dp}{dt} \quad (2.9)$$

$$\Rightarrow \frac{b}{V} \cdot \frac{dp}{dt} \text{ Joules} \quad (2.10)$$

In unit time within impact - parameter (b) to (b+db) the number of collisions in a unit volume between electrons and ions is,

$$\frac{1}{t} \text{ sec} = n_i \times n_e \times V \times 2\pi b \quad db \quad (2.11)$$

Total power emitted by the electrons in that time is from (2.10)

$$dp = 2\pi b^2 n_i n_e \frac{dp}{dt} db \text{ W/cm}^3 \quad (2.12)$$

Substituting $\frac{dp}{dt}$ from (2.7)

$$dp = 2\pi b^2 n_i n_e \frac{Z^2 e^6}{96 \pi^3 \epsilon_0^3 c^3 m_e^2 b^4} db \text{ W/cm}^3 \quad (2.13)$$

Total bremsstrahlung power emitted in a unit volume can be obtained by integrating (2.13), from b_{\min} i.e. compton wavelength to b_{\max} i.e. ∞ .

The compton wavelength is given by

$$b_{\min} = h/2\pi m_e V$$

Total power emitted from a unit volume of plasma is

$$P = \frac{Z^2 e^6 n_i n_e V}{24\pi \epsilon_0^3 c^3 m_e h} \text{ W/cm}^3 \quad (2.14)$$

Substituting the characteristic electron velocity 'V' by mean thermal velocity,

$$V = \left[\frac{8 K T_e}{\pi m_e} \right]^{1/2} \quad (2.15)$$

$$P = \frac{Z^2 e^6 n_i n_e}{24\pi \epsilon_0^3 c^3 m_e h} \left[\frac{8 K T_e}{\pi m_e} \right]^{1/2} \text{ W/cm}^3 \quad (2.16)$$

$$\text{which gives } P = 1.69 \times 10^{-32} n_e n_i T_e^{1/2} \text{ W/cm}^3 \quad (2.17)$$

where T_e is in eV, densities are in $\# \text{ cm}^{-3}$.

The total bremsstrahlung radiation from the plasma when there are ions of different species can be given by,

$$P = 1.69 \times 10^{-32} n_e T_e^{1/2} \sum_i n_i Z_i^2 \text{ W/cm}^3 \quad (2.18)$$

Calculation of $\sum_i n_i Z_i^2$:

In the plasma, carbon (impurity) exist in 7 different states. Hydrogen (impurity), D & T (fuel) exist in 2 different states.

In Ref. 14 Post et al have reported polynomial fit data for 47 elements to compute $\sum_i n_i Z_i^2$, as a function of electron temperature ($0.002 \text{ KeV} \leq T_e \leq 100 \text{ KeV}$). These data are generated

using a "coronal equilibrium" model, i.e. the distribution of charge state of any ion is governed by the equilibrium between electron impact ionization and recombination.

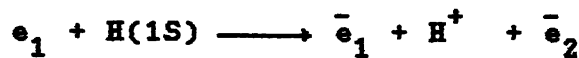
The polynomial fit is given by:

$$\langle Z^2 \rangle = \sum n_i z_i^2 = \sum_{i=0}^5 c(i) \left[\log_{10} T_e (\text{KeV}) \right]^i \quad (2.19)$$

$c(i)$ are available for 47 elements ($26 \leq Z \leq 92$) in [14] in a temperature range of ($0.002 \text{ KeV} \leq T_e \leq 100 \text{ KeV}$).

$\sum n_i z_i^2$ for carbon is calculated using this fit.

To calculate $\sum_I n_i z_i^2$ for hydrogen, again coronal equilibrium model is considered. Electron impact ionization (EII) for hydrogen is



and the radiative recombination (RR) for hydrogen is as follows:



The rate of these reactions are

$$\langle \sigma \cdot v \rangle_{\text{EII}} n_e n_{H(1S)} \text{ for EII and } \langle \sigma \cdot v \rangle_{\text{RR}} n_e n_{H^+} \text{ for RR.}$$

Assuming coronal equilibrium, i.e. an equilibrium between EII and RR [16]

$$\langle \sigma \cdot v \rangle_{\text{EII}} n_e n_{H(1S)} \cong \langle \sigma \cdot v \rangle_{\text{RR}} n_e n_{H^+} \quad (2.20)$$

$$n_{H(1S)} = \frac{\langle \sigma \cdot v \rangle_{\text{RR}}}{\langle \sigma \cdot v \rangle_{\text{EII}}} n_{H^+} \quad (2.21)$$

Further since n_H = total hydrogen density is the sum of $n_{H(1S)}$ and n_{H^+} or

$$n_H = n_{H(1S)} + n_{H^+} \quad (2.22)$$

$$n_{H^+} = \frac{n_H}{\left[1 + \frac{\langle \sigma \cdot V \rangle_{RR}}{\langle \sigma \cdot V \rangle_{EII}} \right]} \quad (2.23)$$

$$\text{and } n_{H(1S)} = (n_H - n_{H^+}) \quad (2.24)$$

$\langle \sigma \cdot V \rangle_{EII}$ for hydrogen is calculated from polynomial fits in reference [15]

$$\ln \langle \sigma \cdot V \rangle = \sum_{n=0}^8 b_n \ln (T_e)^n \quad (2.25)$$

b_n are available in [15], for a temperature range 0.1 eV to 20 KeV. $\langle \sigma \cdot V \rangle_{RR}$ for hydrogen is calculated from the semi-empirical relation in [15].

For $n \equiv nl = 1S; 2S; 2P;$

$$\langle \sigma \cdot V \rangle_{RR} = A_{nl} \times 10^{-14} \left[E_n^{\text{ion}} / Ry \right]^{1/2} \frac{\beta_n^{3/2}}{\beta_n + X_{nl}} \text{ cm}^3/\text{sec} \quad (2.26)$$

where $Ry = \text{Rydberg constant} = 13.58 \text{ eV}$

$T = \text{Maxwell temperature.}$

$$\beta_n = E_n^{\text{ion}} / T$$

	nl	1S	2S	2P
A_{nl}		3.92	2.47	6.22
X_{nl}		0.35	0.12	0.61

For $n \geq 3$

$$\langle \sigma \cdot V \rangle_{RR} = 5.201 \times 10^{-14} \beta_n^{3/2} E_1(\beta_n) \exp(\beta_n) \text{ cm}^3/\text{sec.} \quad (2.27)$$

$E_1(\beta_n) = \text{exponential integral.}$

In the code developed only transition from 2S to 1S is considered.

So now, (2.23) and (2.24) is solved to obtain population of different stages of hydrogen from where $\sum_i n_i z_i^2$ for hydrogen is obtained.

Calculation of $\sum_i n_i z_i^2$ for D & T is done assuming no existence of D & T neutrals in the plasma. This is because the total number of D & T is very high of the order of 10^{14} (for 'ADITYA' design), in comparison to D^0 , T^0 (neutrals) at high temperatures (> 10 KeV) [14]. So to save computation time without any significant error, in the calculation here existence of D & T neutrals is neglected in the code.

2.2.2 Cyclotron Radiation [3,17]

While bremsstrahlung is a process that takes place within the short time an electron spends in the vicinity of an ion or atom, cyclotron emission is a non-collisional mechanism that occurs in the interval - between collisions. It originates from the orbital acceleration of an electron in a magnetic field. Cyclotron emission by ions is insignificant because of their large mass.

For electrons whose energies are less than several hundred electron volts, cyclotron emission is concentrated in a single spectral line, whose radiation frequency ω equals the orbital frequency, ω_b ($\omega_b = eB/m$, B = strength of magnetic field).

A gyrating electron in a strong magnetic field (Fig.2.4) with characteristic frequency ' ω ' emits photon because of centripetal acceleration [13]. The radiated power of a relativistic electron is given by [3], equation (2.3)

$$\omega = \frac{eB}{m_e} (1 - v^2/c^2)^{1/2} \quad (2.28)$$

In terms of this relativistic gyrofrequency, the velocity and acceleration of the electron may be written as

$$\dot{\underline{V}} = \omega \underline{V} \quad (2.29)$$

where $\dot{\underline{V}}$ = acceleration, for gyro motion is perpendicular to \underline{V} . So for a single electron from (2.3),

$$\frac{dp}{dt} = \frac{e^2 \omega^2 v_{\perp}^2}{6\pi \epsilon_0 c^3 (1 - v_{\perp}^2/c^2)} \text{ watts} \quad (2.30)$$

Substituting for ω in (2.30)

$$\frac{dp}{dt} = \frac{e^4 v_{\perp}^2 B^2}{6\pi \epsilon_0 c^3 m_e^2 (1 - v_{\perp}^2/c^2)} \text{ watts} \quad (2.31)$$

Total power radiated by all electrons from unit volume of plasma is, n_e times the radiated power in eq. (2.31). The electron in a plasma of fusion interest will have a Maxwellian distribution; of perpendicular velocities. Integrating over such a Maxwellian distribution from [3].

$$P = \frac{e^4 B^2 n_e}{3\pi \epsilon_0 m_e^2 c} \left(\frac{K T_e}{m_e c^2} \right) \left[1 + \frac{5K T_e}{2m_e c^2} + \dots \right] \text{ W/cm}^3 \quad (2.32)$$

This can be approximated to [18].

$$P = 6.21 \times 10^{-28} B^2 n_e T_e \text{ W/cm}^3 \quad (2.33)$$

where

B is in Gauss

n_e is in cm^{-3}

T_e in eV.

The photons which are emitted in cyclotron radiation from fusion plasma have very high frequencies approximately 100 GHz [3]. In fusion condition plasma densities (10^{14} cm^{-3}) and temperatures (10 ~ 20 KeV) such high frequencies photons are reabsorbed. Such photons are also perfectly reflected from the first wall. Reflectivities at such high frequencies are nearly 0.98 or even higher [3]. Since most of the cyclotron radiations are absorbed in the plasma and because of a high reflectivity, it is very difficult to estimate the exact amount that escapes to the wall. Here in the present model it is assumed that only 2 percent of the total cyclotron radiation is reaching the wall.

2.2.3 Charge Exchange Neutrals

Charge exchange is a process where redistribution of particles takes place



Here an electron goes from atom 'A' to the ion ' B^+ '. The electron transition from the atom 'A' to the ion ' B^+ ' is accompanied by transfer of the momentum ' mv ', where m = electron mass and v = relative velocity of the nuclei of 'A' and ' B^+ '. This process occurs in a plasma and leads to significant loss of

energy from the plasma. The charge exchange neutrals move quite fast and dump their energy at the wall surface.

Out of the various charge exchange reactions possible in the plasma, some significant contributions comes from the reaction



The rate of other reactions are very small [19]. So only the above reaction is considered as a source of charge exchange neutrals formation.

Rate of the above reaction is given as

$$R_{CX} = n_{H^+} n_{H^0} \langle \sigma \cdot V \rangle_{CX} \quad (2.34)$$

The factor n_{H^+} and n_{H^0} calculations are described in detail in section 2.2.1.

From [15], polynomial fits are available to compute $\langle \sigma \cdot V \rangle_{CX}$, as a function of temperature T of the plasma particle and energy E of the incident particle

$$\ln \langle \sigma \cdot V \rangle = \sum_{i=0}^8 \sum_{j=0}^8 a_{ij} (\ln E)^i (\ln T)^j \quad (2.35)$$

The coefficient a_{ij} are available in [15]. These fits are valid in the range $0.1 \text{ eV} < E < 20 \text{ KeV}$ and $0.1 \text{ eV} < T < 20 \text{ KeV}$. Energy of these charge exchanged neutrals are very high approximately 1.5 times the ion-temperature in the plasma.

So in terms of energy, the amount generated from unit volume of plasma, because of CX neutrals is

$$P_{CX} = n_{H^0} n_{H^+} \langle \sigma \cdot V \rangle_{CX} \cdot (1.5) T_i \text{ W/cm}^3 \quad (2.36)$$

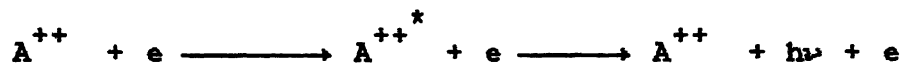
where $T_i = \text{Joules}$.

2.2.4 Line Radiations

Atomic line radiations can be divided into three categories [3]:

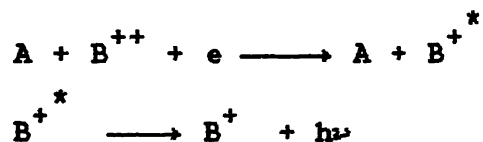
(i) Ordinary spectral line radiation

Ordinary spectral line radiation occurs when an electron is excited to a higher state by electron impact. It usually de-excites in a very short time 10^{-7} sec by the process of an emission of a photon.



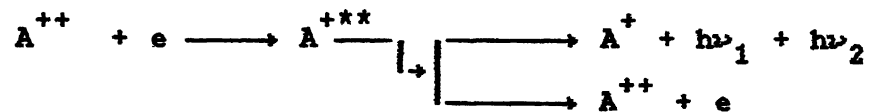
(ii) Radiative recombination :

Radiative recombination occurs as a result of a capture of a free electron by an ion with a third body in the vicinity. Binding energy of the electron is radiated when it falls to ground state



(iii) Dielectronic Recombination

Dielectronic recombination involves capture of a free electron with excitation of a orbital electron at the same time, such that both electrons are in excited state



There are two ways in which the doubly excited atom can decay.

(i) either it will give rise to two spectral lines (dielectronic recombination) or

(ii) ionized with the release of an electron (autoionization)

The autoionization process is very fast on the order of 10^{-13} S, so only dielectronic recombination is of interest.

Atomic line radiation can not be emitted from completely stripped ions of the light element fuels of fusion interest; but it can occur from incomplete ionized or neutral of high Z impurity.

In this model, line radiations from impurities (carbon and hydrogen) is only considered.

Line radiations from hydrogen:

In case of hydrogen, out of the three processes discussed above, spectral line emission and radiative recombination is possible.

Spectral line emission:

Reference [18] gives empirical relation for spectral line emission radiation estimation.

For a transition from $n \longrightarrow m$,

$$I_{nm} = 5.1 \times 10^{-25} \frac{f_{nm} g_1 n_e n_o}{g_m T_e^{1/2}} \left(\frac{\Delta E_{nm}}{\Delta E_{n1}} \right)^3 \exp \left(- \frac{\Delta E_{n1}}{T_e} \right) \text{ W/cm}^3 \quad (2.37)$$

where f_{nm} = oscillator strength,

g_m = statistical weight of m^{th} state ($m=1$, ground state)

T_e in eV

n_o = neutral density

$$\Delta E_{nm} = E_n - E_m$$

To make the model simpler only transitions to ground state ($m=1$)

are considered from $n = 2$ to 6 only.

So

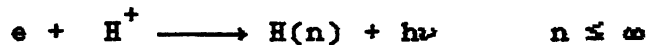
$$I_{n1} = 5.1 \times 10^{-25} \frac{f_{n1} n_e n_o}{T_e^{1/2}} \exp \left[-\frac{\Delta E_{n1}}{T_e} \right] \quad (2.38)$$

The oscillator strength f_{n1} ($n = 2$ to 6) are available in [15] and from [18],

$$\Delta E_{n1} = 13.6 \left[1 - \frac{1}{n^2} \right] \quad (2.39)$$

Radiative recombination:

The radiative recombination process is as follows:



only ground state ($n=1$) is considered in this model.

Rate of this reaction is

$$R = n_e n_{H^+} \langle \sigma \cdot V \rangle \quad (2.40)$$

Calculation of $\langle \sigma \cdot V \rangle$ for this reaction is given in (2.26).

Further energy of the photon released in this reaction is

$$E_{h\nu} = E_e + \frac{Ry}{n^2} \quad (2.41)$$

Ry = Rydberg constant = 13.58 eV.

Energy released from unit volume of plasma through this process is thus,

$$E = n_e n_{H^+} \langle \sigma \cdot V \rangle \left[E_e + \frac{Ry}{n^2} \right] \text{ W/cm}^3 \quad (2.42)$$

Line radiations from carbon:

Post et al in Ref. [14] have given polynomial fits for radiative cooling rates in a temperature range of 0.002 KeV-100

KeV for 47 elements $2 \leq Z \leq 92$.

Cooling rate i.e. cooling rate per free electron in $\text{ergs/cm}^3 \text{ sec.}$ is given by

$$\log_{10} L_Z = \sum_{i=0}^5 A(i) \left\{ \log_{10} [T_e (\text{KeV})] \right\}^i \quad (2.43)$$

where $A(i)$ are available in [14].

The energy loss rate in $\text{ergs/cm}^3 \text{ sec.}$ can be found by multiplying the cooling rate by electron density and ion density.

These fits include effects of all the three types of line radiations.

2.2.5 Fusion Neutrons

Fusion neutrons are the main source of loading among all sources considered, each time a deuterium and tritium fuses a neutron of high energy (14.5 MeV) is released.



These neutrons cause extensive damage to the first wall.

Rate of this fusion reaction is

$$R = n_D \cdot n_T \langle \sigma \cdot V \rangle_{DT} \quad (2.44)$$

From [16], the coefficient $\langle \sigma \cdot V \rangle_{DT}$ is given by

$$\langle \sigma \cdot V \rangle_{DT} = \frac{3.68 \times 10^{-12}}{T_e^{2/3} (\text{KeV})} \exp \left[- \frac{19.94}{T_e^{1/3} (\text{KeV})} \right] \text{cm}^3/\text{sec} \quad (2.45)$$

So rate of neutron release from unit volume of plasma is given by (2.44), the total energy can be obtained by multiplying this number with energy of each neutrons (14.5 MeV).

2.3 Calculation algorithm for local wall power loading

Because of the toroidal symmetry and uniform property of plasma throughout the torus, (i.e. variations of plasma parameters are same in any part of the torus), it is sufficient to consider a small thickness of the torus for this analysis. Results obtained at any section will be similar; Fig. (2.5).

Assume a small thickness of unit length ($\Delta\phi$) along toroidal direction is cut out. This section can be assumed to be a cylinder having elliptical cross section. This volume is then divided into a number of cells, by drawing concentric ellipses.

The volume of each cell is then calculated, using the following method.

The area of the shaded portion in Fig. (2.6) is given by

$$\Delta A = \left\{ \frac{ab}{2} \tan^{-1} \left[a/b \left[\tan\theta_2 - \tan\theta_1 \right] \right] \right\} \quad (2.46)$$

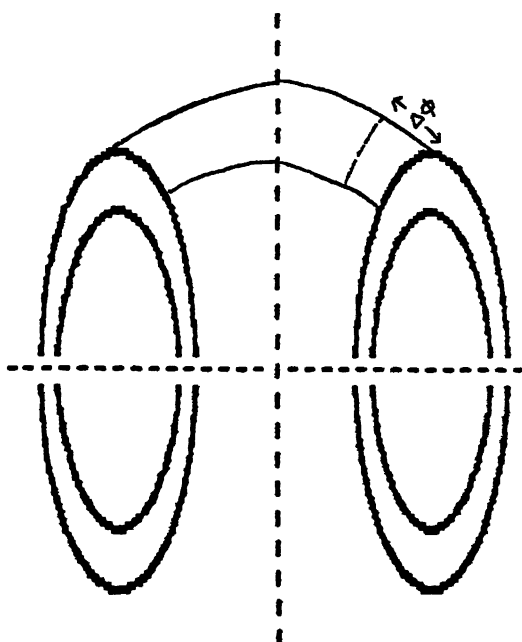


Fig 2.5

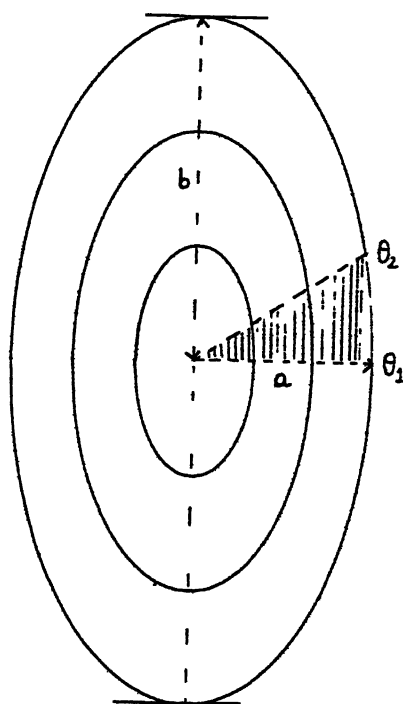


Fig 2.6

So cross sectional area of each of the cells can be determined by subsequent subtraction from each other. Multiplication of these surface areas with $\Delta\phi$ will give volume of each cell.

In section 2.2, analytical formulae are given to compute the radiations in watt/cm³; when multiplied by volume of the cell, that will give total energy radiated from that volume.

Now, to compute the poloidal distribution of the radiation, which impinges on the first wall the following method is used.

Selecting any arbitrary wall point and considering small length ' Δl ' along the poloidal direction of the wall in Fig. (2.7), the fraction of the radiation generated in the cell that will reach Δl is

$$F = \frac{\Delta l \cos \beta}{2\pi (AB)} \quad (2.47)$$

where β = angle between line joining the centre of Δl to centre of the cell and normal to Δl .

$$\beta = \text{Angle (XBA)} - \text{Angle (XBC)} \quad (2.48)$$

Angle (XBC) = 90° , since CB is perpendicular to Δl

$$\text{Angle (XBA)} = \frac{\text{slope of } (\overline{AB}) - \text{slope of } (\overline{XY})}{1 + \text{slope of } (\overline{AB}) \times \text{slope of } (\overline{XY})} \quad (2.49)$$

From each cell the total radiation can be calculated and using (2.48) and (2.49) the fraction of radiation that will reach the defined wall point can be calculated.

So if ' E ' = total radiation from any cell, ' A '.

E_{BA} = fraction of ' E ' which is reaching ' B ' from ' A ' = $F \times E$

E_B = total radiation reaching ' B ', from all cells = $\sum_A E_{BA}$

$$\text{So total energy flux at 'B' } = \frac{\sum E_{BA}}{A \Delta l * \Delta \phi} \text{ watt/cm}^2.$$

2.3.1 Volumetric heat generation terms

The local wall power loadings derived above is then used for temperature solution of the first wall. Out of the various loading discussed, the bremsstrahlung and neutrons causes volumetric heat generation in the first wall. Bremsstrahlung is high energy radiation and is not monoenergetic, but distributed over a wide range of energies. The average photon energy coming out as bremsstrahlung radiation is of the order of the electron temperature [3]. This approximation is used here to calculate the mass absorption coefficient for the wall material, corresponding to bremsstrahlung radiation.

The three main processes, which occur when gamma rays interact with matter are-

1. Photoelectric effect
2. Compton effect
3. Pair production.

Below 1.02 MeV of photon energy, the first two processes are only active [20].

Data for mass absorption coefficients (μ) for photon energy above 1 MeV are available in [21].

For photon energy below 1 MeV, the mass absorption coefficient can be calculated by approximate formulas given in [20].

Photoelectric absorption coefficient,

$$\tau(E) \approx 10^{-33} N Z^2 E^{-3.5} \text{ cm}^{-1} \quad (2.50)$$

Compton absorption coefficient,

$$\sigma(E) \approx 1.25 \times 10^{-25} \frac{NZ}{E \left[\log_e \{2E/mc^2\} + \frac{1}{2} \right]} \text{ cm}^{-1} \quad (2.51)$$

The high energy neutrons (~ 14.5 MeV) generated in the fusion reaction are sufficiently energetic to penetrate through the first wall. They cause most of the heating in the first wall, and damage the first wall. The neutron macroscopic cross-section (Σ) (which is equivalent to mass absorption coefficient in gamma rays) for different material are listed in [23].

The energy flux or intensity of beams (neutrons or gamma rays) I (watt/cm^2) is equal to the product of flux and energy of the particles. For gamma rays $I = \phi (h\nu)$, $h\nu$ = energy per photon, and in the case of neutrons, $I = \phi \Delta E$, ΔE = energy loss per neutron reaction.

In the case of monoenergetic photons or neutrons, I is directly proportional to ϕ , so that I can be written as [24]

$$I(x) = I_0 e^{-\mu x} \quad (2.52)$$

$$I_0 = \text{intensity at } x = 0.$$

From [24], the energy absorbed and consequently the heat generated in a particular location of an absorber where intensity of the radiation is I , is

$$q''(x) = \mu I(x) \quad (2.53)$$

and specifically for neutrons

$$q''(x) = \Sigma \phi(x) \Delta E \quad (2.54)$$

where q'' = volumetric thermal source strength (watt/cm³).

The intensity variation with distance from (2.52) and (2.53) can be derived to be

$$q''(x) = q''_0 e^{-\mu x} \quad (2.55)$$

where q''_0 = volumetric thermal source strength at $x=0$.

2.4 Temperature solution in the first wall

In this section, two methods will be discussed for temperature solution in the first wall, one for the surface heating (cyclotron, charge exchange neutrals, line radiation) and the other one for the volumetric heating terms (neutrons and bremsstrahlung).

Temperature solution for surface heating:

Since a very small portion of the torus is considered for local wall power loading calculations, the first wall of that small portion can be assumed as a solid plate type element. A one dimensional heat flow condition is assumed.

The heat conduction equation for this case (Fig.2.8) is the one dimensional poisson equation,

$$\frac{d^2 t}{dx^2} + \frac{q''}{K} = 0 \quad (2.56)$$

K = thermal conductivity of the first wall material.

Considering a thin layer of thickness Δx at distance x from midplane, the heat crossing plane x is given by

$$q_x = -K A \frac{dt}{dx} \quad (2.57)$$

So

$$t(x) = - \frac{q''}{K} x + c_1 \quad (2.58)$$

Assuming the temperature at $x = L$ (L = thickness) as T_1

$$t(x) = t_1 + \frac{q''}{K} (L - x) \quad (2.59)$$

Temperature solution for volumetric heating:

The case of flat slab is again treated. Fig. (2.9) shows a slab of thickness 'L' subjected to radiation from one side only, resulting in an exponential volumetric source strength distribution. Assuming one dimensional heat flow along positive x direction only. from (2.56)

$$q_x = -K A \frac{dt}{dx}$$

using (2.54)

$$\frac{dt}{dx} = - \frac{q''_0 e^{-\mu x}}{K} \quad (2.60)$$

$$t(x) = \frac{q''_0}{K\mu} e^{-\mu x} + c \quad (2.61)$$

$$\text{At } x = L, t(x) = t_1$$

$$\text{which gives } c = - \frac{q''_0}{K\mu} e^{-\mu L} + t_1$$

$$\text{so } t(x) = t_1 + \frac{q''_0}{K\mu} \left[e^{-\mu x} - e^{-\mu L} \right] \quad (2.62)$$

Calculation of outer wall temperature:

Coolant arrangement for the first wall is already discussed in section 1.5, i.e. coolant tube of the same material as the first wall are attached to the back of the wall and there is only one input and output of the tube. Mass flow rate and input temperature of coolant are known.

Defining a coordinate 's', $0 < s < 2\pi a$, on the perimeter of the coolant tube From general principle of convective heat

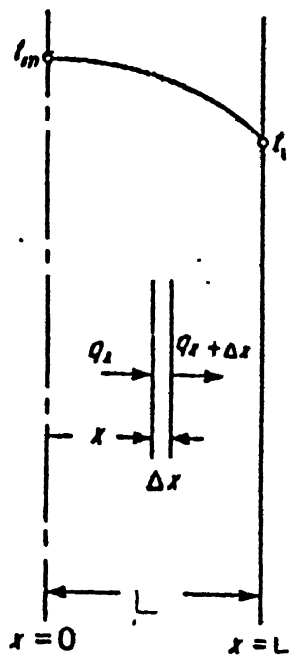


Fig 2.8 Surface heating

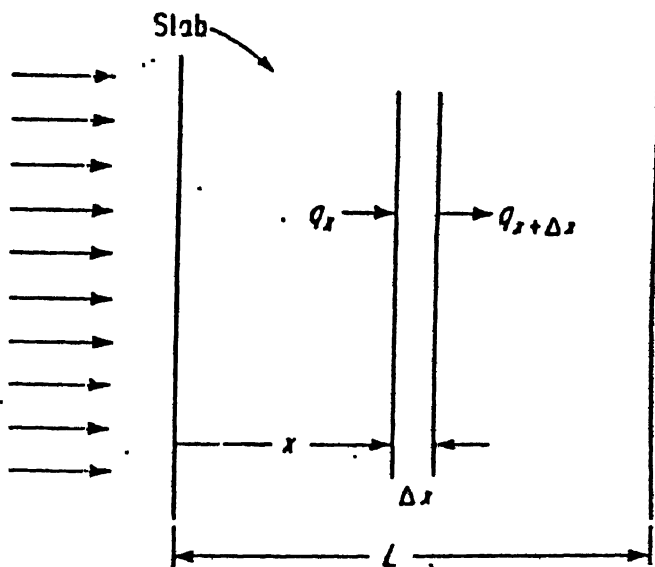
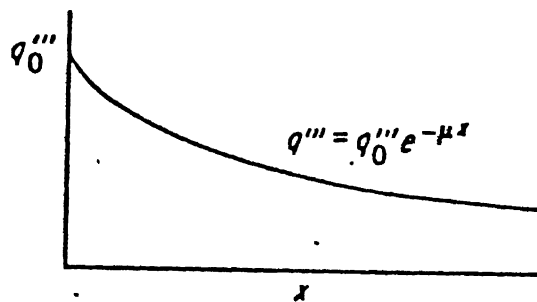


Fig 2.9 Volumetric heating

transfer,

$$\rho C_p (T(s) - T_{in}) A_{xs} u = \text{heat load from plasma between 0 to s} \quad (2.63)$$

where ρ = density of coolant

C_p = specific heat of coolant

A_{xs} = area of cross section of the coolant tube

u = velocity of coolant.

So $T(s)$ = bulk temperature of the coolant at 's' can be solved from (2.63).

Considering a differential element of wall of unit area,

$$h(T_1 - T(s)) = \text{plasma load at s (watt/cm}^2\text{)} \quad (2.64)$$

where h = heat transfer coefficient

which can be obtained from the three dimensionless constants.

Reynold number, Nusslet number and Prandtl number

$$Re = \frac{Du\rho}{\mu} \quad (\text{Reynold number}) \quad (2.65)$$

$$Pr = \frac{C_p \mu}{K} \quad (\text{Prandtl number}) \quad (2.66)$$

$$Nu = 0.023 \times Re^{0.8} \times Pr^{0.4} = \frac{hD}{K} \quad (\text{Nusselt Number}) \quad (2.67)$$

where μ = viscosity of liquid (coolant).

Equation (2.64) gives the outer wall temperature (t_1) of the first wall.

2.5 Limitations and Suggestions

1. It has been assumed that the average photon energy in bremsstrahlung radiation is of the order of electron temperature

of the plasma [3]. Since the bremsstrahlung radiation is one of the major contributor to wall loading, a more accurate method is required to model the volumetric heating caused by bremsstrahlung radiation by splitting it in different energy groups. Method described in Ref. [10] can be implemented for an accurate analysis of the bremsstrahlung energy deposition.

2. For cyclotron emission, it is assumed that due to reflection from the wall and absorption in the plasma, 98% of the cyclotron emission is lost, according to [3]. However this is only a rough estimate. Tamor [3] did a transport analysis of the balance between synchrotron-radiation and reabsorption for cylindrical and toroidal plasmas and found that the plasma core radiates strongly, but the plasma is actually heated near its outer radius, leading to a flatter temperature profile than would otherwise exist. Thus cyclotron radiation, tends to cool the core of fusion plasma and heat the outer periphery of the plasma. A full radiation transport calculation is essential for an accurate estimation of these effects.

3. For the charge exchange neutrals source term, it has been assumed that number of charge exchange neutrals formed at a point, move towards the wall is constant throughout its way upto the wall. Whereas due to further ionization and further charge exchange the number of neutrals formed at a point and the number of neutrals reaching the wall may differ. Detail calculation is required for this attenuation of charge exchange neutrals.

4. Only one dimensional heat conduction is assumed in the

first wall without considering the toroidal shape of the first wall, i.e. by assuming the small portion of the torus a cylinder and the wall is like a flat plate. Inclusion of toroidal geometry (shape factor) in the calculation of temperature will give more close value to the actual case.

CHAPTER 3

SYSTEM CODE FOR FIRST WALL TEMPERATURE CALCULATION

3.1 A Brief Outline about the Code

A code is developed for the first wall temperature calculation of a tokamak reactor. The code is written in 'FORTRAN' language. Model used for the purpose is discussed in Chapter 2.

The code is written in a modular fashion, so that in future, as to requirement, with availability of better formulation, any part can easily be replaced.

Some details about the code is given below:

1. Title of the Code: First wall thermal analysis and temperature calculation in a tokamak reactor.
2. Computer - H.P. 9000
Installation place - I.I.T. Kanpur
3. Operating system - Unix
4. Language used - FORTRAN
5. Number of lines - The main program is connected to 13 link files (subroutines) and data files for polynomial fits. The entire code is ~850 lines (~ 30 Kb).
6. Nature of physical problem - Calculation of all major types of radiations, with most of the parameters are inbuilt within the code, proper polynomial fits are used for this purpose, and based on that the one-dimensional temperature solution of the first wall, with a specific coolant arrangement system.

3.2 Input/Output of the Code

Input to the 'FORTRAN' code includes the following:

The corresponding variables used in the code are shown in bold capitals.

1. Plasma dimensions

- a) Plasma major radius (in cm) 'XMJR'
- b) Plasma minor radius (in cm) 'XMNR'

2. First wall dimensions

- a) Major radius of first wall (in cm) 'XMJRW'
- b) Minor radius of first wall (in cm) 'XMNRW'

3. Density and temperature profiles

The code will assume a flat type density and temperature profile, if 'XOPTION' is set to any number less than 2. For any other value of 'XOPTION', the code will go for a peaked profile. The constant α_n , α_t of profile type, eqn. (2.1,2.3) can be varied, by changing 'ALPHAN' and 'ALPHAT'.

4. Impurity contents

- a) Ratio of, density of hydrogen to density of electron
'HYDIMP'

- b) Ratio of, density of carbon to density of electron
'CARBIMP'

5. Magnetic field strength

- a) Magnetic field strength in 'Gauss' 'BMAG'

6. First wall material

- a) Thickness of first wall material (cm) 'WALLTHICK'
- b) Conductivity of first wall material (W/cm °C) 'THCWALL'

c) Neutron removal cross-section for the first wall material 'XMUE' (This variable appears in Link-12).

7. Coolant tube

a) Thickness of coolant tube wall (cm) 'PIPETHICK'

8. Coolant

The following input informations are required for the coolant. They are dependent on coolant system pressure.

a) Density of coolant (kg/cm^3) 'DENCool'.

b) Viscosity of coolant ($\text{kg}/\text{cm}\cdot\text{sec}$) 'VISCOSITY'

c) Thermal conductivity of coolant ($\text{W}/\text{cm}^\circ\text{C}$) 'THCCool'

d) Inlet temperature of coolant ($^\circ\text{C}$) 'TEMPINCOOL'

9. Wall point position, where the temperature profile is required in degree. 'THETA', THETA = 0 indicates minor axis.

The code performs the following calculations:

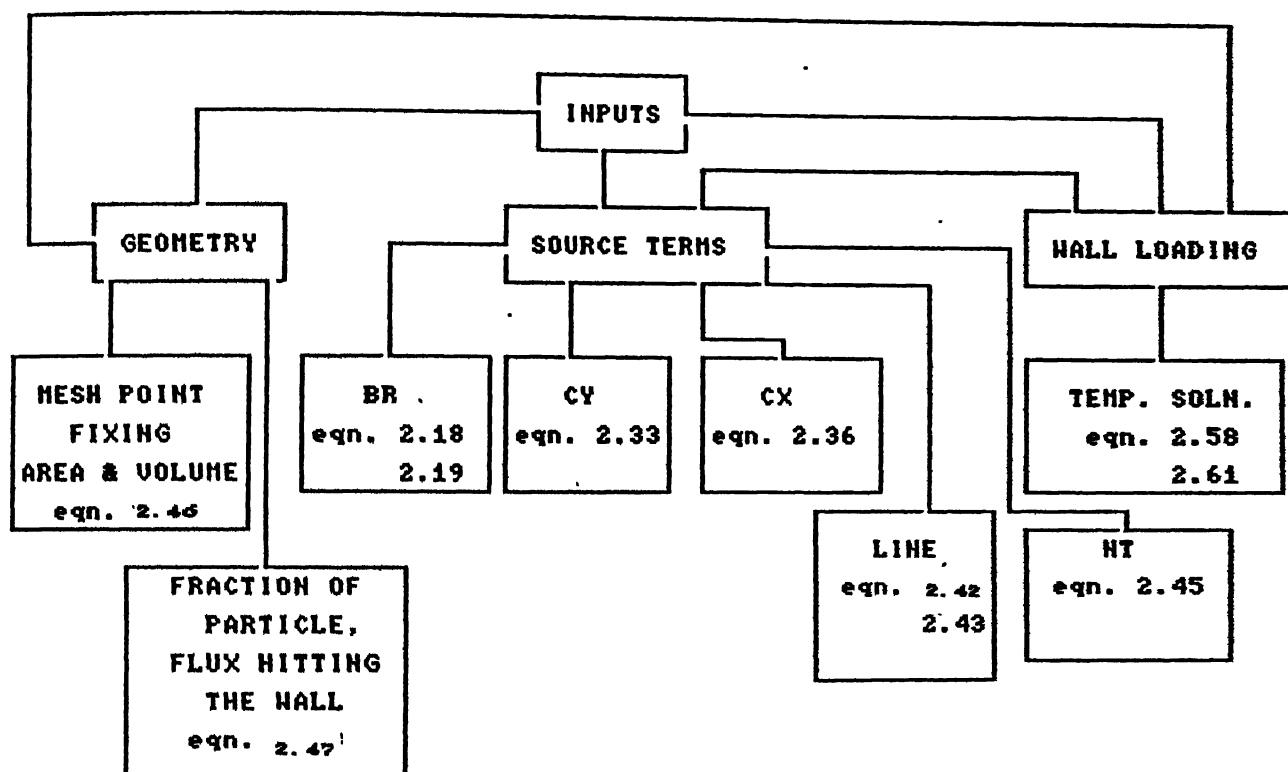
1. The spatial profiles of the intensities of line and recombination radiation, charge exchange, neutrals, bremsstrahlung, cyclotron radiation and fusion neutrons.

2. Fraction of particle flux that hits the wall point of interest.

3. Based on item 1, calculation of the surface and volumetric heat load on the wall as a function of poloidal angle.

4. Calculate the heat transfer coefficient and hence the temperature profile through the wall. The temperature profile at 50 points of the wall are redirected to an output file 'TEMP.DAT'.

3.3 Flow Chart



CHAPTER 4

RESULTS

The code was tested with several sets of input parameters, including the 'ADITYA' parameters. The results shown here are for the following 'ADITYA' parameters. Other parameters, whenever used is indicated separately.

1. Electron temperature = 15 KeV (max)
2. Ion temperature = 15 KeV (max)
3. Electron density = $4 \times 10^{14} \text{ cm}^{-3}$ (max)
4. Ion density = $4 \times 10^{14} \text{ cm}^{-3}$ (max)
5. Magnetic field strength = 1.5 T
6. Plasma minor radius = 30 cm
7. Plasma major radius = 60 cm
8. First wall minor radius = 32 cm
9. First wall major radius = 62 cm
10. Carbon density in plasma = 0.1 x electron density
11. Hydrogen density in plasma = 0.1 x electron density
12. Thickness of first wall = 2 cm
13. First wall material = S.S. 314
14. Coolant tube material = S.S. 314
15. Coolant tube wall thickness = 0.5 cm
16. Coolant tube diameter = 1.0 cm.
17. Mass flow rate of coolant = $90.7 \times 10^{-4} \text{ Kg/cm}^2\text{-Sec}$
18. Coolant is ordinary water.
19. Inlet temperature of coolant = 20°C

The poloidal distribution of the total flux at the inside surface of the first wall (facing the plasma) both for flat

profile and peaked profile is shown in fig 4.1 and fig 4.2 respectively. It is seen from the curve that the loading is maximum at $\theta = 90$ (θ = poloidal angle) and $\theta = 270$ for both type of profiles. The distribution of the flux is symmetrical about the major axis.

Flat type profile:

Maximum value of flux = 86.150 watt/cm^2 at $\theta = 90$ & 270

Minimum value of flux = 49.498 watt/cm^2 at $\theta = 0$ & 180

Peaked type profile:

Maximum value of flux = 67.623 watt/cm^2 at $\theta = 90$ & 270

Minimum value of flux = 34.277 watt/cm^2 at $\theta = 0$ & 180

The poloidal distribution of temperature at the inside surface of first wall (facing the plasma) for both flat and peaked profile is shown in fig 4.3 and fig 4.4 respectively. As expected from fig 4.1 and fig 4.2 the maximum temperature is at $\theta = 90$ and 270 and the minimum temperature is at $\theta = 0$ and 180 .

Flat type profile :

Maximum temperature = 832.682°C at $\theta = 90$ & 270

Minimum temperature = 505.008°C at $\theta = 0$ & 180

Peaked type profile :

Maximum temperature = 670.600°C at $\theta = 90$ & 270

Minimum temperature = 371.523°C at $\theta = 0$ & 180

The temperature profile of the first wall at one of the hottest point ($\theta = 90$) is shown for the flat and peaked type profile in fig 4.5 and fig 4.6 respectively.

Flat type profile :

At ($x = 0$ cm) surface facing the plasma Temp. = 832.682

At ($x = 2$ cm) surface away from the plasma Temp. = 568.366

Peaked type profile :

AT ($x = 0$ cm) surface facing the plasma Temp. = 670.600

At ($x = 2$ cm) surface away from the plasma Temp. = 459.836

Fig 4.7 to fig 4.10 shows the variation of source term strength with electron temperature. Fig 4.11 shows the variation of the source term (charge exchange neutrals) with ion temperature. These results are for the same parameter set given above except the impurity levels. Which is assumed as :

The ratio of density of carbon to density of electron in the plasma = 0.01

The ratio of density of hydrogen to density of electron in the plasma = 0.01

Fig 4.7 shows the variation of bremsstrahlung radiation (watt/cm^3) with the electron temperature. As expected from eq.2.18 the variation is proportional to square root of electron temperature. Fig 4.8 shows the variation of cyclotron radiation (watt/cm^3) against the electron temperature. As expected from eq.2.33 the variation is linear.

Fig 4.9 shows the variation of line radiation with electron temperature. Line radiation is low as expected, because at these high temperatures impurities are almost fully ionized, i.e there are no bound electrons. In reality there will be a small radiating region near the edge where the temperature is low.

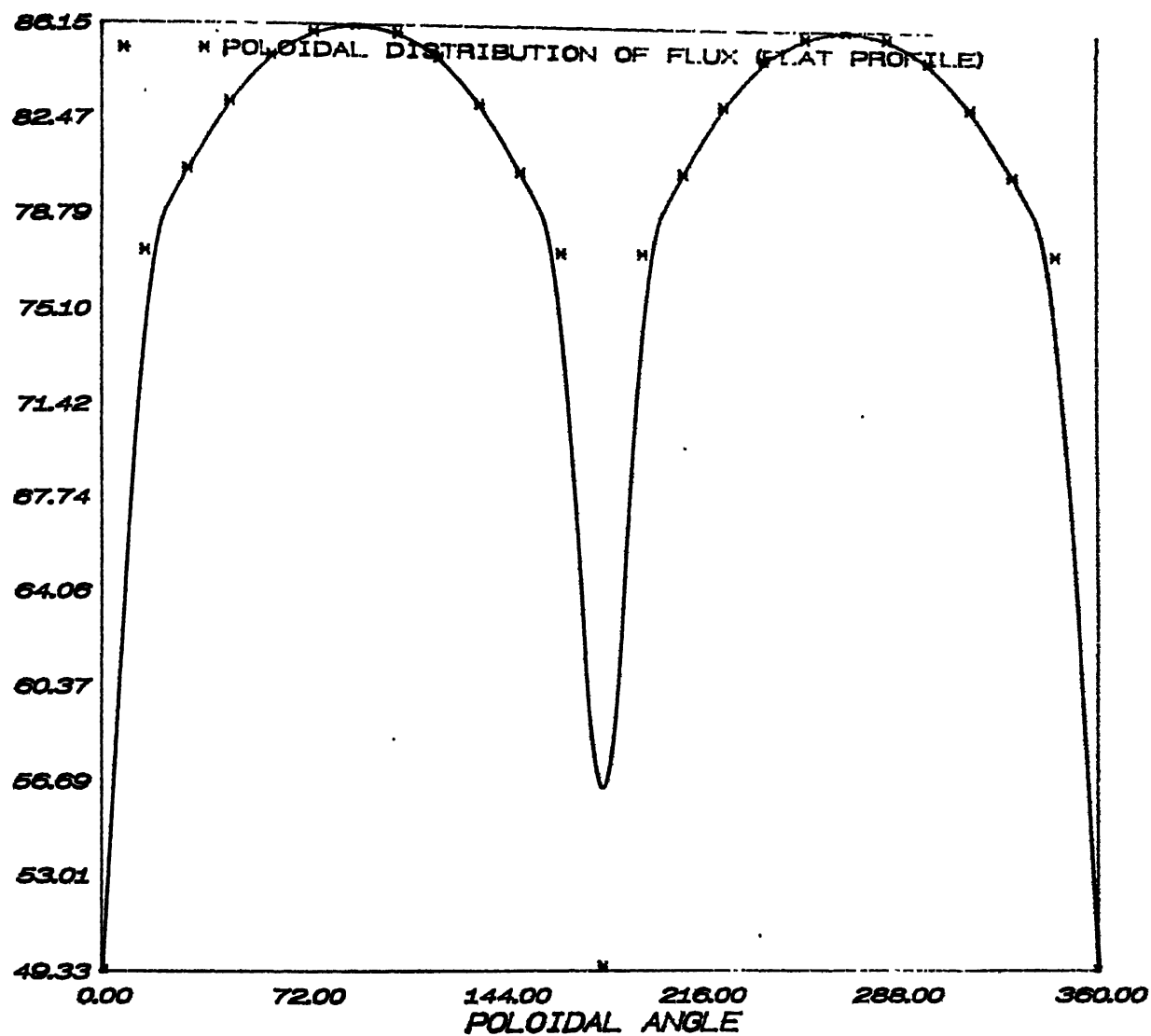


Fig. 4.1 Poloidal distribution of total flux at the inside surface of first wall (flat profile)

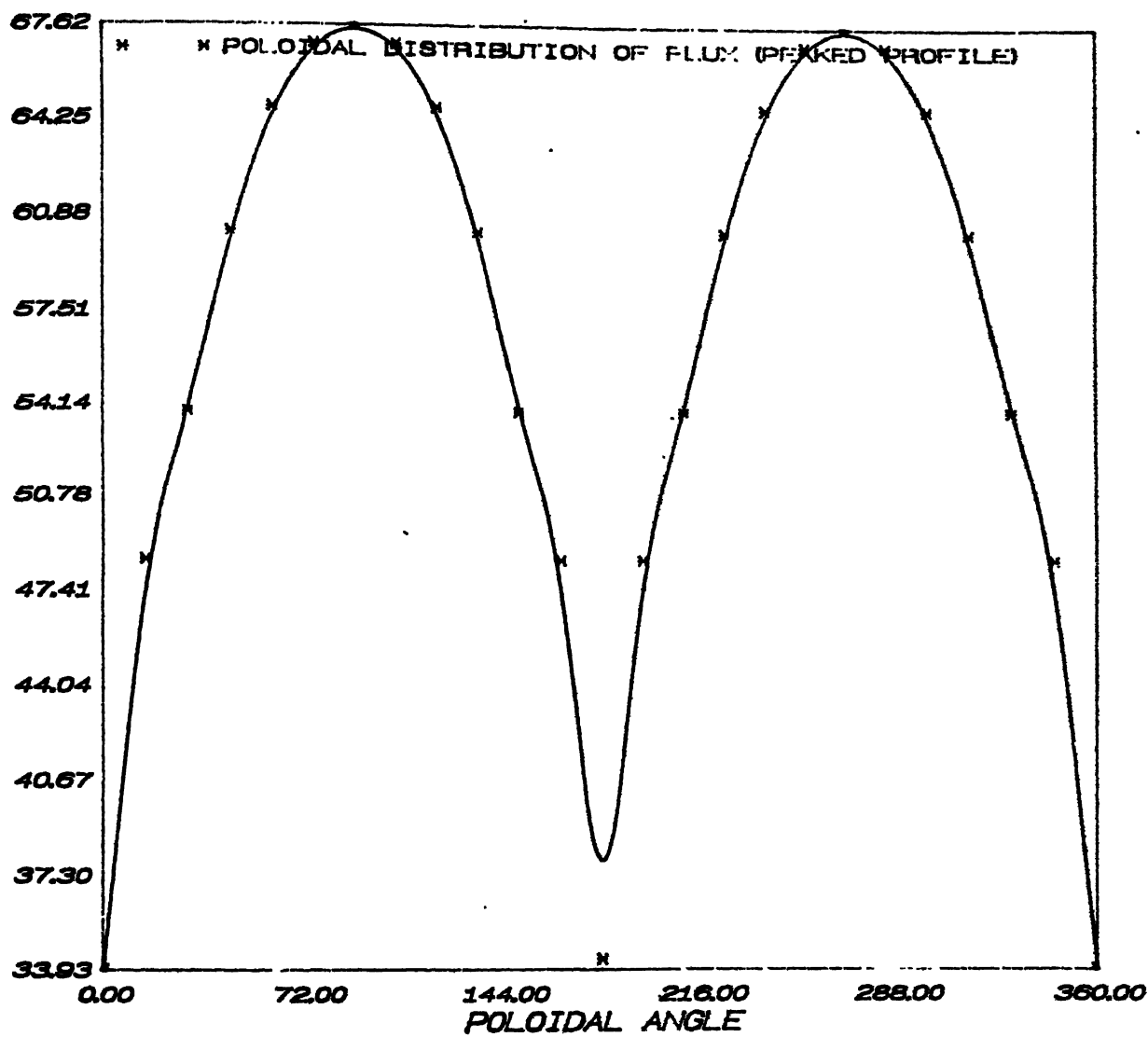


Fig. 4.2 Poloidal distribution of total flux at the inside surface of first wall (peaked profile)

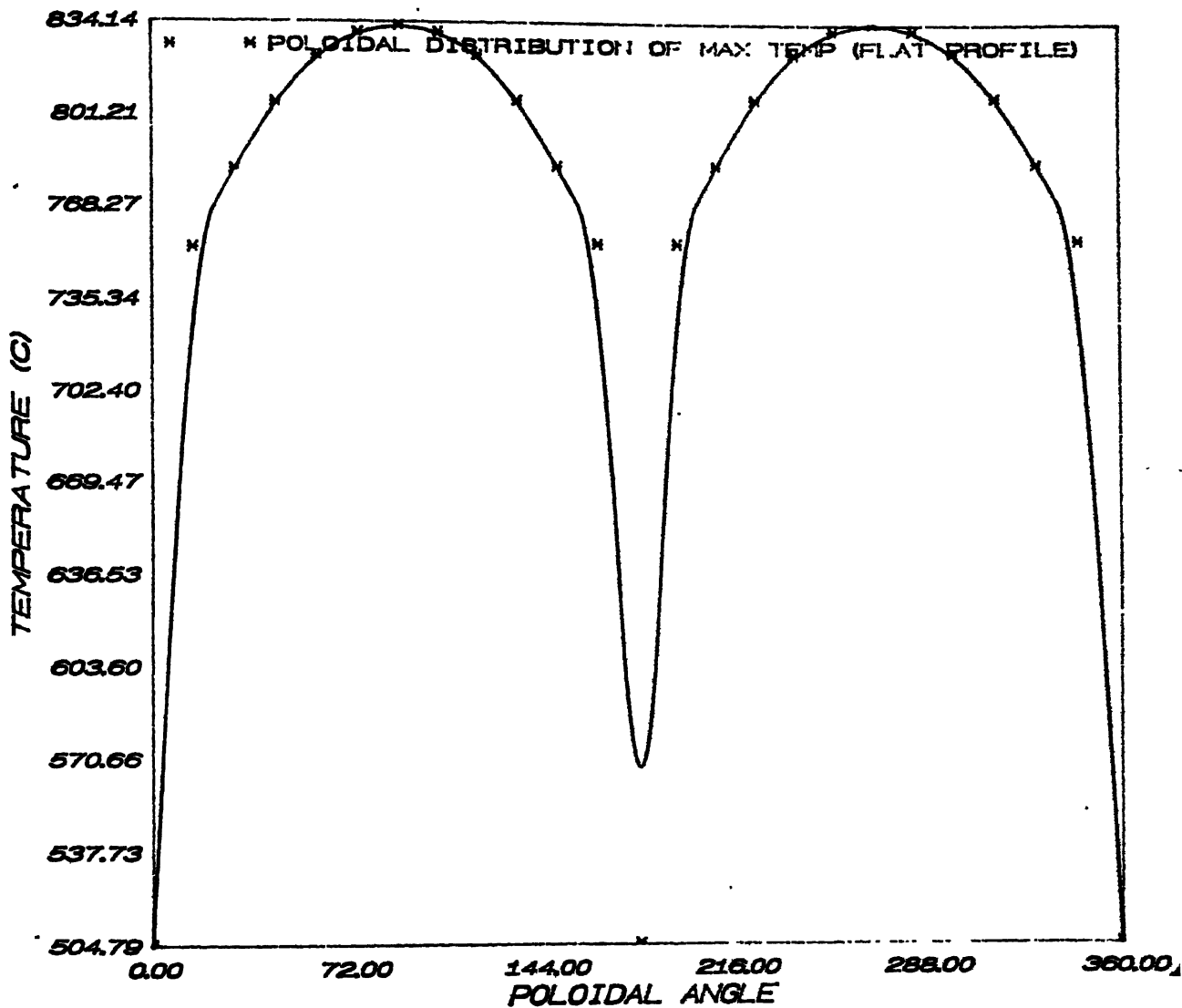


Fig. 4.3 Poloidal distribution of maximum temperature inside surface of first wall (flat profile)

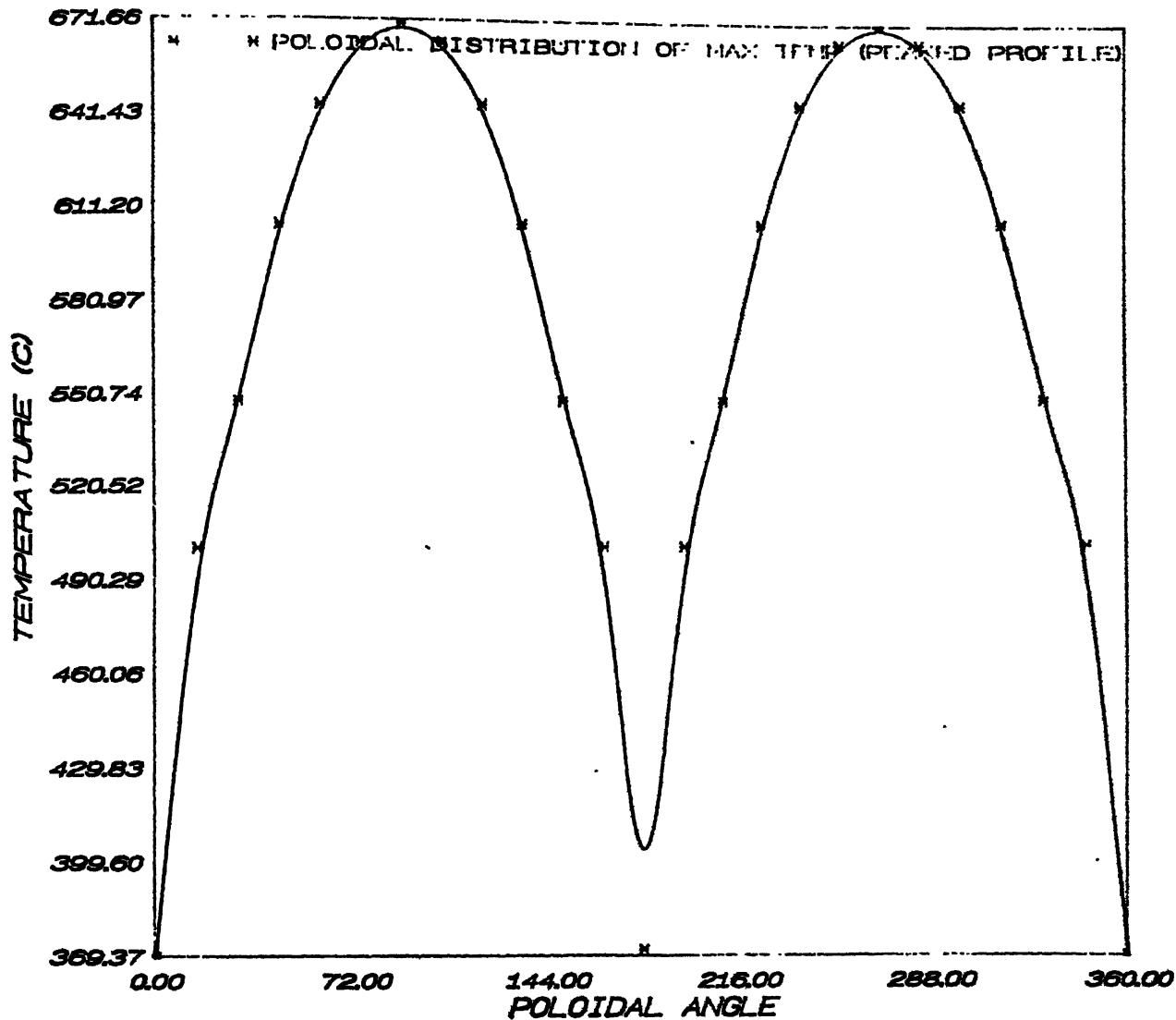


Fig. 4.4 Poloidal distribution of maximum temperature at the inside surface of first wall (peaked profile)

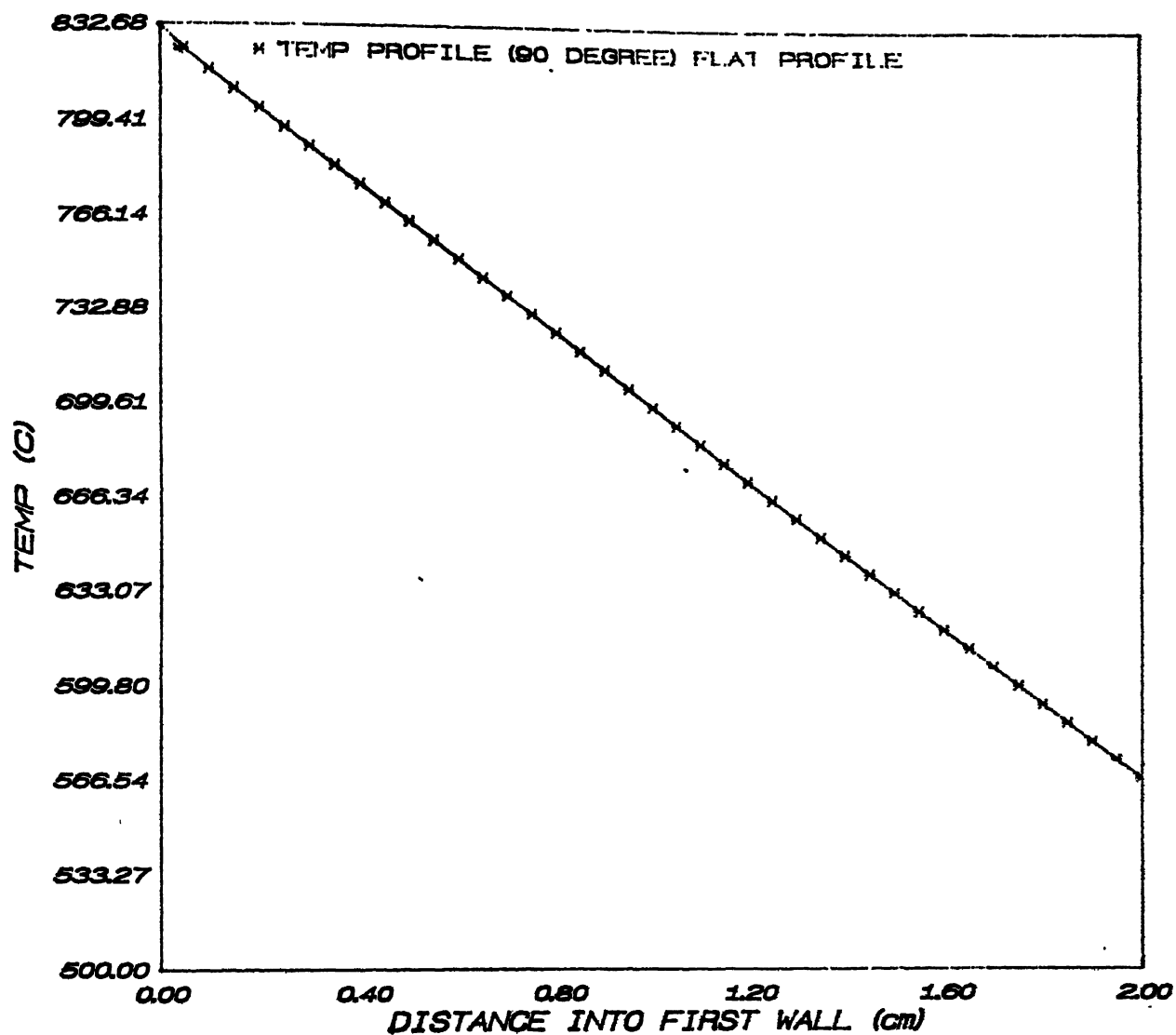


Fig. 4.5 Temperature profile at the hottest point of the wall
(flat profile)

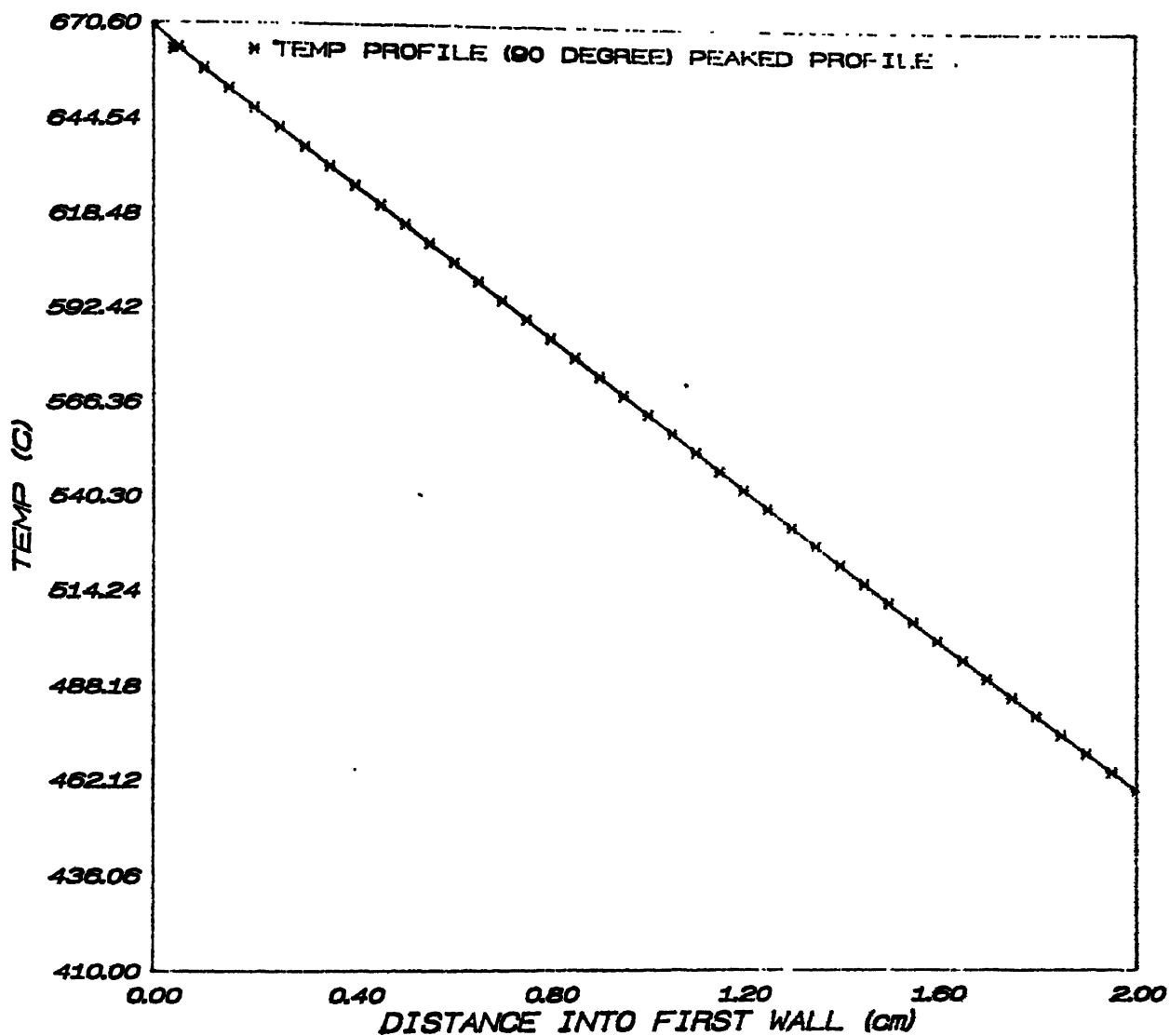


Fig. 4.6 Temperature profile at the hottest point of the wall
(peaked profile)

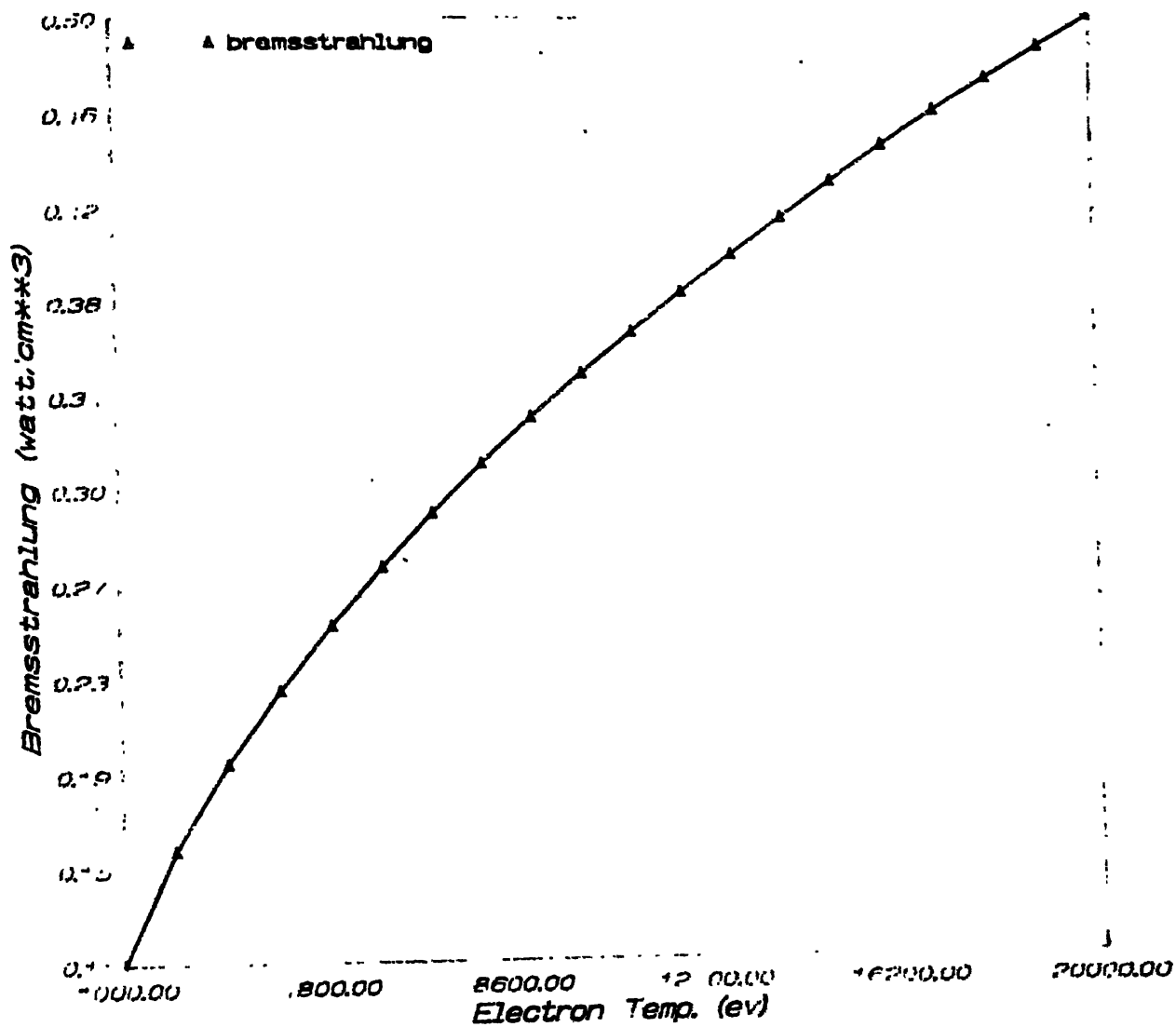


Fig. 4.7 Variation of bremsstrahlung radiation (watt/cm^3) with electron temperature.

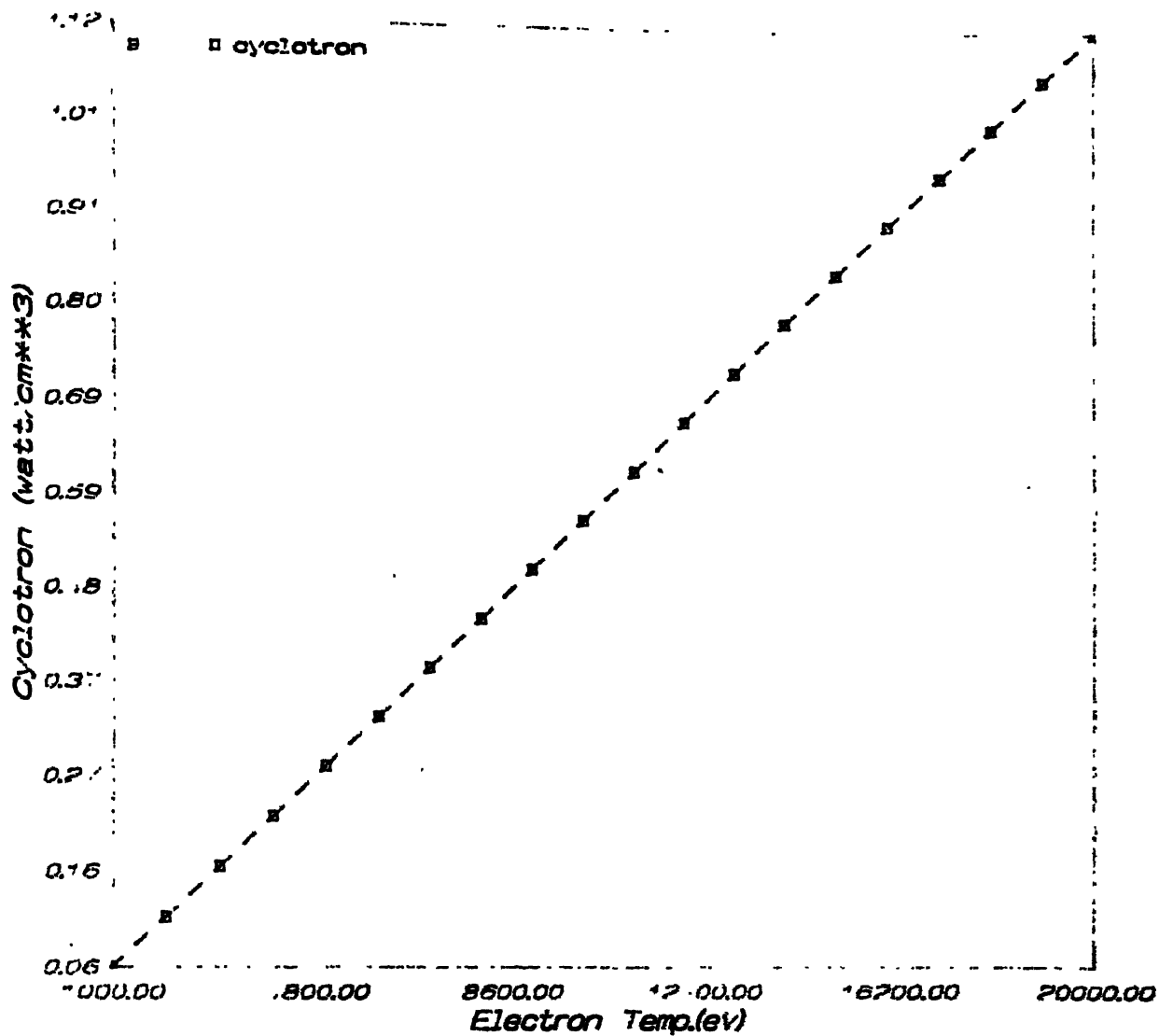


Fig. 4.8 Variation of cyclotron radiation (watt/cm³) with electron temperature.

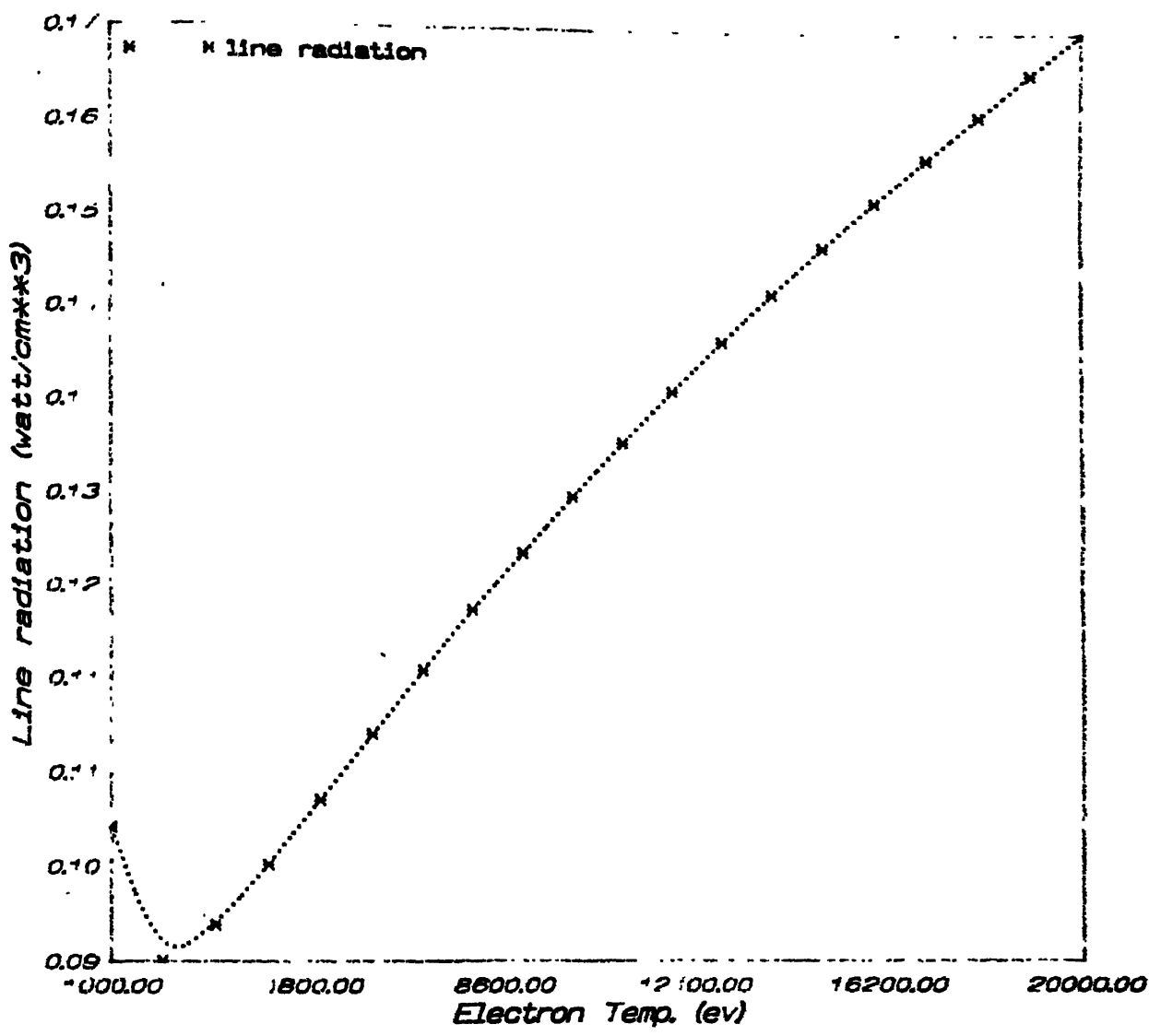


Fig. 4.9 Variation of line radiation (watt/cm³) with electron temperature.

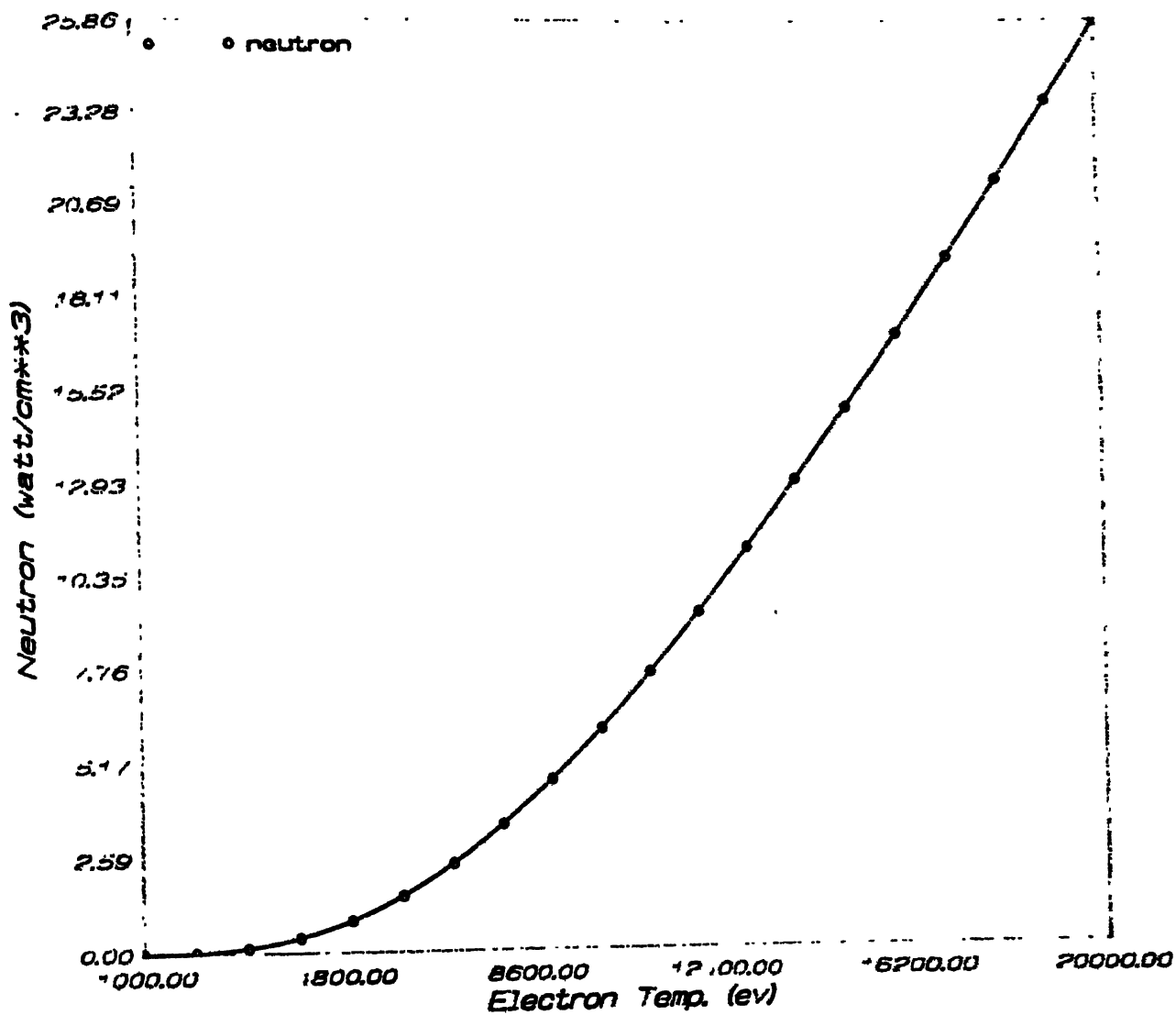
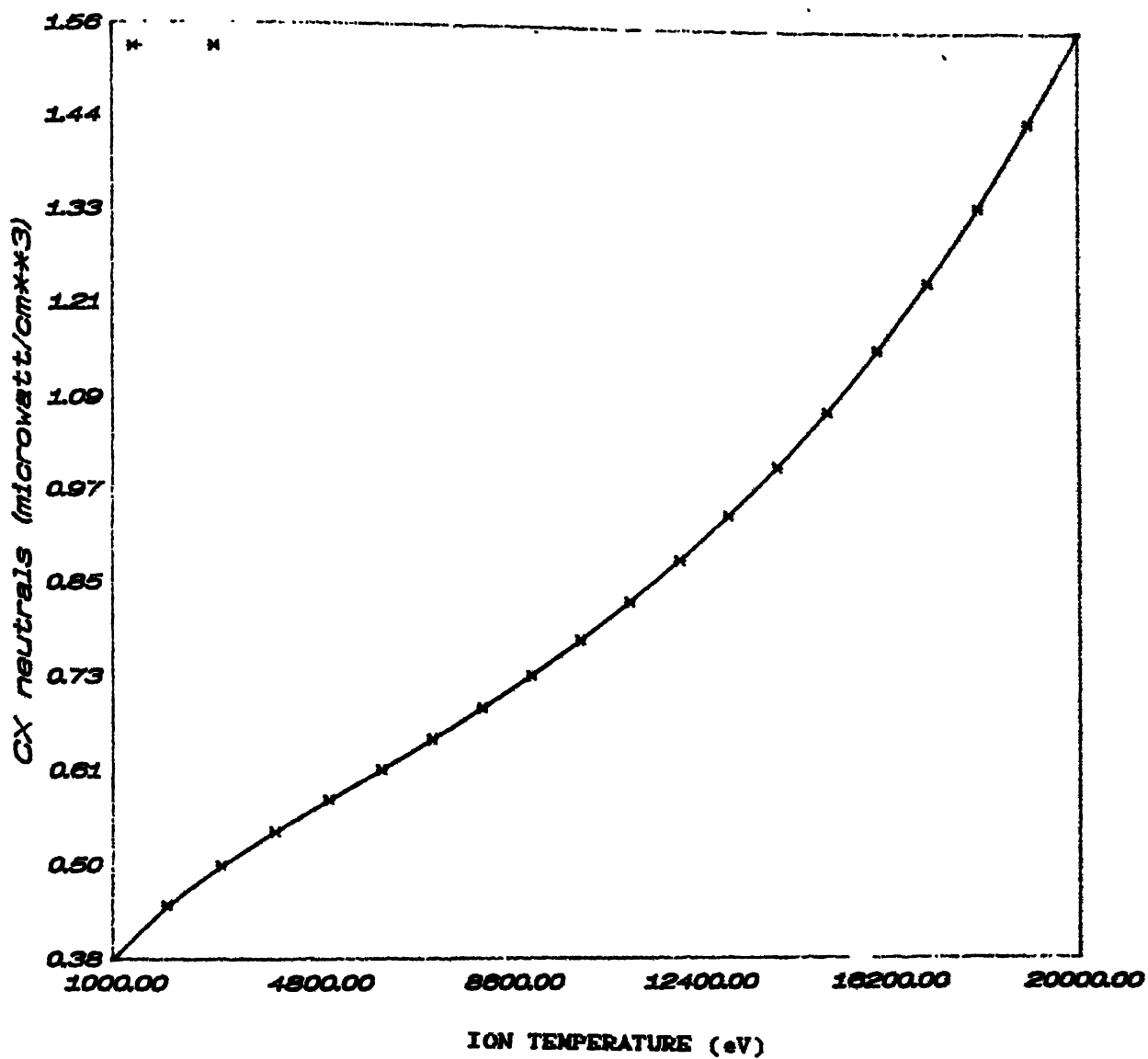


Fig. 4.10 Variation of neutron radiation (watt/cm³) with electron temperature.



g. 4.11 Variation of charge exchange neutrals energy with ion temperature.

Fig 4.10 shows the variation of neutron radiation with the electron temperature. It is seen from the figure that neutron source term increases with increase of electron temperature. That is because the rate of fusion reaction increases with temperature. Also this is seen that among all the source terms the maximum contribution is coming from the neutron term.

Fig 4.11 shows the variation of charge exchange neutrals source term with the ion temperature. This source term is very low as expected, because at such high temperature the recombination reaction rates which are responsible for neutrals formation is small. Since it is assumed that energy carried by the neutrals is 1.5 times the ion temperature the curve shows a increase tendency with increase in ion temperature.

The code is tested with variation of some important parameters and corresponding source terms (watt/cm^3) is shown in table 4.1 to table 4.4. Only the shown parameter is varied and other parameter for these results are as given for "ADITYA".

Table 4.1 shows the density variation of electron (ion density is same as electron density). corresponding strength of source terms are tabulated. As expected all the terms show an increase in value with increase in density.

Table 4.2 shows the variation of electron temperature and corresponding strength of source terms. With increase in electron temperature all the source terms strength increases. Table 4.3 shows the variation of impurities level. Except cyclotron all other terms are affected. Since with increase of impurity the amount of D and T reduced i.e. because electron density and ion

density is fixed, so neutron contribution which is dependent on the density of D and T reduces.

Table 4.4 shows the variation of magnetic field strength and it is seen that only cyclotron radiation is affected by this which was expected.

TABLE 4.1
VARIATION OF THE SOURCE TERMS WITH THE ELECTRON DENSITY

E DENSITY	BR	CY	CX	LINE	NT
0.20E+14	0.107E-02	0.838E-03	0.268E-08	0.375E-03	0.373E-01
0.40E+14	0.430E-02	0.167E-02	0.107E-07	0.150E-02	0.149E+00
0.60E+14	0.968E-02	0.251E-02	0.241E-07	0.337E-02	0.336E+00
0.80E+14	0.172E-01	0.335E-02	0.430E-07	0.600E-02	0.598E+00
0.10E+15	0.269E-01	0.419E-02	0.672E-07	0.937E-02	0.934E+00
0.12E+15	0.387E-01	0.503E-02	0.967E-07	0.135E-01	0.134E+01
0.14E+15	0.527E-01	0.586E-02	0.131E-06	0.183E-01	0.183E+01
0.16E+15	0.688E-01	0.670E-02	0.172E-06	0.240E-01	0.239E+01
0.18E+15	0.871E-01	0.754E-02	0.217E-06	0.303E-01	0.302E+01
0.20E+15	0.107E+00	0.838E-02	0.268E-06	0.375E-01	0.373E+01

E.DENSITY=Electron density ($\#/cm^3$)

BR= Bremsstrahlung radiation ($Watt/cm^3$)

CY= Cyclotron radiation ($Watt/cm^3$)

CX= Charge Exchange neutrals ($Watt/cm^3$)

LINE= Line radiation ($Watt/cm^3$)

NT= Neutron radiation ($Watt/cm^3$)

TABLE 4.2
VARIATION OF THE SOURCE TERMS WITH ELECTRON TEMPERATURE

E.TEMP.	BR	CY	CX	LINE	NT
0.20E+04	0.157E+00	0.223E-02	0.444E-06	0.898E-01	0.249E-01
0.40E+04	0.222E+00	0.447E-02	0.536E-06	0.974E-01	0.410E+00
0.60E+04	0.272E+00	0.670E-02	0.614E-06	0.108E+00	0.345E+01
0.80E+04	0.314E+00	0.894E-02	0.692E-06	0.118E+00	0.345E+01
0.10E+05	0.351E+00	0.111E-01	0.779E-06	0.128E+00	0.608E+01
0.12E+05	0.385E+00	0.134E-01	0.881E-06	0.137E+00	0.929E+01
0.14E+05	0.415E+00	0.156E-01	0.100E-05	0.146E+00	0.129E+02
0.16E+05	0.444E+00	0.178E-01	0.115E-05	0.153E+00	0.170E+02
0.18E+05	0.471E+05	0.201E-01	0.133E-05	0.161E+00	0.213E+02
0.20E+05	0.497E+00	0.223E-01	0.156E-05	0.168E+00	0.258E+02

E.TEMP.=Electron temperature (ev)

BR=Bremsstrahlung radiation (Watt/cm³)

CY=Cyclotron radiation (Watt/cm³)

CX= Charge Exchange neutrals (Watt/cm³)

LINE=Line radiation (Watt/cm³)

NT= Neutron radiation (Watt/cm³)

TABLE-4.3

VARIATION OF THE SOURCE TERMS WITH MAGNETIC FIELD STRENGTH

BMAG	BR	CY	CX	LINE	NT
0.10E+05	0.430E+00	0.745E-02	0.107E-05	0.150E+00	0.199E+02
0.20E+05	0.430E+00	0.298E-01	0.107E-05	0.150E+00	0.149E+02
0.30E+05	0.430E+00	0.670E-01	0.107E-05	0.150E+00	0.149E+02
0.40E+05	0.430E+00	0.119E+00	0.107E-05	0.150E+00	0.149E+02
0.50E+05	0.430E+00	0.186E+00	0.107E-05	0.150E+00	0.149E+02

BMAG=Magnetic field strength

BR=Bremsstrahlung radiation (Watt/cm³)CY=Cyclotron radiation (Watt/cm³)CX=Charge Exchange neutrals (Watt/cm³)LINE=Line radiation (Watt/cm³)NT=Neutron radiation (Watt/cm³)

TABLE 4.4
VARIATION OF SOURCE TERMS WITH IMPURITY CONTENTS

HIMP	CIMP	BR	CY	CX	LINE	NT
0.1E-01	0.1E-03	0.33E+00	0.16E-01	0.103E-05	0.15E-02	0.16E+02
0.1E-02	0.1E-02	0.34E+00	0.16E-01	0.107E-07	0.17E+02	0.17E+02
0.1E-03	0.1E-01	0.43E+00	0.16E-01	0.107E-09	0.15E+00	0.15E+02

HIMP=Hydrogen density /Electron density

CIMP=Carbon density /Electron density

BR=Bremsstrahlung radiation (Watt/cm³)

CY=Cyclotron radiation (Watt/cm³)

CX=Charge Exchanged neutrals (Watt/cm³)

LINE=Line radiation (Watt/cm³)

NT=Neutron radiation (Watt/cm³)

REFERENCES

1. S. Chaturvedi, Studies of a low gain tokamak fusion breeder, IPR/TR-42/91, IPR, Bhat, Gandhinagar, India.
2. John Wesson, Tokamaks, Oxford Engineering Science Series-20 Publication, Oxford (1987).
3. J. Reece Roth, Introduction to fusion energy, Ibis Publishing Charlottesville (1986).
4. Robert A. Gross, Fusion Energy, John Wiley & sons, New York (1984).
5. Terry Kamash, Fusion Reactor Physics, Principles and Technology, Ann-Arbor Science Publishers, Ann-Arbor (1975).
6. George H. Miley, Fusion Energy Conversion, American Nuclear Society, Hinesdale (1976).
7. S. Chaturvedi, Tokamak based fissile fuel breeder, Research and Development Requirements, IPR/TR-40/91, Bhat, Gandhinagar, India.
8. A. Nicolai and D. Reiter, Journal of Computational Physics, 55, 129-153 (1984).
9. M. C. Carrol and G. H. Miley, Fus. Tech, 10 (1986), 770-775.
10. M. C. Carrol, An analytical model for first wall temperature calculations, Ph. D. Thesis, Mech. Engineering. Dept., University of Illinois, Urbana-Champaign (1986).
11. A. Nicolai and P. Borner, Fus. Tech., 12 (July-1987), 119-135.
12. Nicholas A. Krall and Alvin W. Trivelpiece, Principles of

- Plasma Physics, Mc-Graw Hill Book Company, New York (1973).
13. Kenro Miyamoto, Plasma Physics for Nuclear Fusion, M.I.T Press, Cambridge (1987).
 14. D. E. Post et al. , Atomic and Nuclear Data Tables , 20, 397-439 (1977).
 15. R. K. Janev, Langer Jr., D. E. Post Jr, Elementary processes in hydrogen, helium plasmas, Cross sections and reaction rate coefficients, Springer-Verlag, Berlin (1981).
 16. S. Chaturvedi, Basic Plasma Physics Lecture Notes, I.P.R Library, Bhat, Gandhinagar, India (Dec 1990).
 17. G. Bekeffi, Sanborn C. Brown, Americal Journal of Physics, 29, 404 (1961a).
 18. N.R.L. Report, Naval Research Laboratory, U.S., N.R.L 0084/4040.
 19. Sobelman, Vainshtein, Yukov, Excitation of atom and broadning of spectral lines, Springer Verlag, Berlin (1981).
 20. K. Sri Ram, Nuclear Measurements techniques, East West Press (1986).
 21. Theodore Rockwell III, Shielding Manual, D. Van Nostrand Company INC., Princeton, New Jersey (1956).
 22. John R. Sern Goldberg, Nuclear Cross Sections, National Associated Universities INC, Brookhaven (May-1964).
 23. El Wakil, Nuclear Power Engineering, New York, Mc Graw Hill